

Development and Application of a Custom Algorithm to Assess Hamstring Muscle Stiffness

By

David Harrison

July 2020

Director of Thesis: Dr. Zachary J. Domire

Department of Kinesiology

Hamstring strain injuries (HSI) are the most diagnosed musculoskeletal injury among elite international track & field athletes. HSIs appear to occur most often during terminal swing phase of sprinting, placing track & field sprinters and jumpers at high risk of musculoskeletal injury. Repetitive uninterrupted bouts of eccentric loading movements, such as sprinting, can develop sites of microscopic damage within muscle fibers, acting as the origin of future muscular injury. It is unknown if the microscopic damage, occurring from repetitive sprinting movements, can be quantifiable via imaging technologies.

Ultrasound shearwave elastography (SWE) is new imaging tool used to evaluate muscular tissue in vivo. However, the financial burden of this equipment can leave research labs with only a single machine, potentially limiting data collections and the ability to efficiently process data. Development of a custom SWE image processing algorithm will allow for data processing to be completed away from the ultrasound machine, resulting in the ability to perform more data collections. The purpose of this thesis is to develop and validate a custom image processing code and then implement that code to process a pre-existing dataset.

Our custom image processing algorithm was validated successfully against the ultrasound machine in muscle, tendon, and ligament tissues, yielding excellent inter-day intraclass correlation coefficient (ICC) reliability values and excellent standard error measurement (SEM)

values. We reported ICC (SEM) values of 0.999 (0.01 kPa), 0.999 (0.22 kPa), and 0.998 (0.46 kPa) for muscle, tendon, and ligament, respectively.

Validated custom image processing algorithm was applied to a pre-existing dataset tracking hamstring muscle stiffness of track & field athletes. An outlier analysis revealed one participant suffered a grade I HSI, 55.69 kPa, 5.45 standard deviations above the mean. Ten more outlier data points were reported ranging 2.1-4.86 standard deviations above the mean values; however, these ten data points did not result in a diagnosed muscular injury.

This thesis successfully created a custom SWE image processing algorithm that can be utilized to assess stiffness in muscle, tendon, or ligament tissue. Our preliminary results reveal we can quantify and track changes in muscle material properties and regular monitoring of athletes can help identify those individuals at risk of muscular strain via SWE stiffness assessment.

Development and Application of a Custom Algorithm to Assess Hamstring Muscle Stiffness

A Thesis

Presented to the Faculty of the Department of Kinesiology

East Carolina University

In Partial Fulfillment of the Requirements for the Degree

The Masters of Science in Kinesiology

Biomechanics Concentration

By

David Harrison

July 2020

© 2020, David Harrison

DEVELOPMENT AND APPLICATION OF A CUSTOM ALGORITHM TO ASSESS
HAMSTRING MUSCLE STIFFNESS

By

David Harrison

APPROVED BY:

DIRECTOR OF THESIS: _____
Zachary J. Domire, PhD

COMMITTEE MEMBER: _____
Anthony S. Kulas, PhD

COMMITTEE MEMBER: _____
Patrick M. Rider, MS

CHAIR OF THE DEPARTMENT
OF KINESIOLOGY: _____
Joonkoon Yun, PhD

DEAN OF THE
GRADUATE SCHOOL: _____
Paul J. Gemperline, PhD

TABLE OF CONTENTS

LIST OF TABLES	vii
LIST OF FIGURES	viii
CHAPTER I. INTRODUCTION.....	1
Statements of Purpose.....	4
Hypotheses	5
Significance.....	5
Delimitations	6
Limitations	7
CHAPTER II. REVIEW OF LITERATURE	8
Introduction.....	8
Prevalence of Hamstring Strain Injury	8
Hamstring Strain Injury Mechanisms.....	10
Eccentric Contraction and Exercise Effect on the Hamstring Muscle Complex	13
Musculoskeletal Elastography Imaging.....	15
Summary	20
CHAPTER III. METHODS.....	21
Introduction.....	21
Exclusion Criteria.....	21
Participants.....	22
Equipment and Instrumentation	23
Measurement Protocol.....	24

Data Processing	25
Pilot Testing of MATLAB Algorithm.....	30
Statistical Analysis	31
Reliability Analysis of Custom Image Processing Algorithm.....	31
Validation Analysis of Custom Image Processing Algorithm.....	31
Analysis of Pre-existing Dataset	31
CHAPTER IV. RESULTS	34
Reliability of Custom Algorithm.....	34
Validation of Algorithm Against the Ultrasound Machine.....	34
Hamstring Stiffness Gender Differences: Day One Data	36
Previous HSI History vs. No HSI History: Day One Data	37
Outlier Analysis of Individual Participant Hamstring Stiffness	40
Tracking Individual Participant Hamstring Stiffness Throughout Competitive Season	42
Tracking Mean Hamstring Stiffness Throughout Competitive Season.....	45
CHAPTER V. DISCUSSION	50
Introduction.....	50
Established Reliability of Custom Algorithm.....	50
Validated Custom Algorithm	51
Hamstring Stiffness Gender Differences	52
HSI History vs. No Previous HSI History	52
Individual Participant Outlier Analysis	53
Tracking Hamstring Stiffness Throughout Competitive Season	54
Seasonal Effect on Mean Hamstring Stiffness.....	55

Areas for Future Research	56
Limitations	57
Conclusion	58
REFERENCES.....	59
APPENDIX A: INDIVIDUAL PARTICIPANT HAMSTRING STIFFNESS PLOTS	67
APPENDIX B: DEMOGRAPHICS QUESTIONNAIRE.....	76
APPENDIX C: INFORMED CONSENT DOCUMENT	78
APPENDIX D: CUSTOM ALGORITHM FLOWCHART	81
APPENDIX E: IRB APPROVAL LETTER	83

LIST OF TABLES

Table 1: Participant Demographics.....	22
Table 2: Participant Injury History and Events Competed in.....	23
Table 3: Changes to Pixel Intensity Values After Equation 1 is Applied.....	27
Table 4: Pilot Data Results.....	30
Table 5: Absolute and Relative Mean Differences Between Algorithm and Ultrasound Machine	35
Table 6: Biceps Femoris Stiffness Across Measurement Days (kPa).....	46
Table 7: Semitendinosus Stiffness Across Measurement Days (kPa)	46
Table 8: Semimembranosus Stiffness Across Measurement Days (kPa)	46
Table 9: Percent Differences Between Measurement Day 1 and Day 4 Means	47

LIST OF FIGURES

Figure 1: SWE elastogram of hamstring muscle	24
Figure 2: Plotted RGB color bar data.....	25
Figure 3: SWE elastogram superimposed over b-mode image	26
Figure 4: Normalized image after image opacity setting is accounted for.....	27
Figure 5: Pilot data elastograms.....	30
Figure 6: De-identified Muscle Images Bland-Altman Plot.....	35
Figure 7: De-identified Tendon Images Bland-Altman Plot	36
Figure 8: De-identified Ligament Images Bland-Altman Plot	36
Figure 9: Gender Stiffness Differences within Individual Hamstring Muscles	37
Figure 10: HSI History vs. No HSI History and Its Impact on Muscle Stiffness.....	39
Figure 11: Stiffness Differences in Biceps Femoris Muscle at Separate Locations	40
Figure 12: Stiffness Differences in Semitendinosus Muscle at Separate Locations.....	41
Figure 13: Stiffness Differences in Semimembranosus Muscle at Separate Locations.....	41
Figure 14: Individual Participant Left Biceps Femoris Mid-Belly Stiffness Changes Throughout Competitive Season.....	42
Figure 15: Individual Participant Right Biceps Femoris Proximal Stiffness Changes Throughout Competitive Season.....	43
Figure 16: Individual Participant Right Semimembranosus Mid-Belly Stiffness Changes Throughout Competitive Season	43
Figure 17: Individual Participant Right Semimembranosus Proximal Stiffness Changes Throughout Competitive Season	44
Figure 18: Mean Biceps Femoris Muscle Stiffness Throughout Competitive Season	47

Figure 19: Mean Semitendinosus Muscle Stiffness Throughout Competitive Season48

Figure 20: Mean Semimembranosus Muscle Stiffness Throughout Competitive Season49

Chapter I. Introduction

Among elite track & field athletes, musculoskeletal thigh injuries are the most common injury type, accounting for 52.9% of all reported muscle injuries during elite international athletics over an eight year period (Edouard et al., 2016). During international track & field competitions hamstring strain injury (HSI) is the most documented injury, accounting for 15.7% of all injuries (Alonso et al., 2012; Crema et al., 2018; Edouard et al., 2016). Hamstring muscles experience large amounts of re-injury also. Re-injury rates, reported by the Australian Football League (AFL), indicate injury recurrences reached as high as 26% for HSIs (J. W. Orchard et al., 2013). Epidemiological data from professional European footballers reported 13% of documented hamstring strains ended up being identical injury recurrences within 2 months of initial return to play (Ekstrand, Waldén, et al., 2016). High rates of recurrent injuries are also causing increased time missed from trainings and competitions; HSIs resulted in an average of 21 missed matchers per club per season during 3 AFL seasons (J. Orchard & Best, 2002). The amount of time missed due to HSIs has financial implications among sports also. A time-loss duration of only 14 days, on average, can be as costly as 250,000 euros and \$96,000 per HSI for professional European Football and the National Football League, respectively (Ekstrand, Waldén, et al., 2016; Elliott et al., 2011).

Exact injury mechanics of HSIs vary within research literature. The consensus among researchers is that HSIs are acute in nature and result from large force magnitudes. In contrast, it has been postulated that the initial event that may lead to a muscle strain injury is caused by microscopic damage to muscle fibers (Friden et al., 1983; Wood et al., 1993). Previous research in-situ animals suggest that muscles stretched to only 30% of their maximum length causes strain to the muscle that is equal to a clinically diagnosed “low grade” muscular strain (Noonan et al.,

1994). In the same study, passive stretch of muscle fibers can lead to insufficient energy absorption capabilities or small structural defects (weak points) within the muscle (Noonan et al., 1994). It is also hypothesized that recurrent performance of eccentric contractions of the hamstring group, i.e. sprinting during training/practice and competition or any sporting event that requires repetitive explosive running, may result in multiple areas of microscopic damage in the hamstrings (C. L. Brockett et al., 2001; Clark, 2008). Research literature suggests HSIs occur during the terminal swing phase of the sprinting gait cycle (Heiderscheit et al., 2005; Schache et al., 2009, 2012; Thelen, Chumanov, Best, et al., 2005). Cause of damage appears to be a result of non-uniform lengthening of sarcomeres and the amount of active strain these muscle fibers accumulate during repetitive eccentric contractions (Lieber & Fridén, 1993; Morgan, 1990). Previous research found that increasing amounts of accumulated active muscle strain, from repetitive eccentric contraction, causes HSIs (Garrett, 1990). Continued repetitive eccentric loading to the sites of disrupted fibers act as a focal point for future damage, potentially lead to a more severe strain injury (Proske & Morgan, 2001).

We postulate that the accumulated microscopic damage caused from repetitive eccentric loading may be quantifiable with advancements in imaging technology. Considering the high injury prevalence, increased re-injury rates, time missed from trainings and competitions, and the substantial financial burden associated with HSIs, clinicians and researchers should be focused on identifying an athlete's potential for injury. Research exists showing ultrasound B-mode imaging to be as useful as MRI in assessment of hamstring muscle strains lesions (Connell et al., 2004). However, B-mode imaging is limited by its inability to quantify the microscopic changes occurring within musculoskeletal tissue. Development of protocols allowing researchers and

clinicians to assess musculoskeletal structure changes on a localized level is an important area for future research.

Shear wave elastography (SWE) shows promise in allowing clinicians and researchers to assess microscopic alterations in skeletal muscle. SWE has the potential to help improve diagnosis, treatment, and investigation into injury mechanisms of skeletal muscle (Yoshitake et al., 2014). A study conducted by Yoshitake et al., 2014 showed the capability to consistently measure shear elastic modulus of muscle between trials and between days, reporting intra-class correlational values as high as 0.978 and 0.948, respectively. It should be noted, processing of shear modulus to determine mean stiffness values was performed using the built-in Q-box software on the ultrasound machine (Nordez & Hug, 2010; Yoshitake et al., 2014). However, the Q-box software limited researchers in their selection of region of interest dimensions, restricted region of interest shape to a circle, and only allowed for a maximum of three regions of interest to be analyzed per SWE image. These factors may become problematic for researchers imaging soft tissue structures differing in architectural size and shape.

A shear wave elastography image processing custom algorithm potentially is less limiting than the Q-box software currently used on the ultrasound machine. A custom code will permit researchers to create regions of interest of any shape and size to best fit the structures being processed and the user will be able to place as many region of interests as they need for processing. Equally significant, a custom processing code is not only more time efficient but previous research groups, Gatos et al., 2016, have established it can be equally reliable in evaluation of shear modulus when compared to the Q-box software. Recently, custom algorithms for shear wave image processing have become more readily implemented because of programs such as MATLAB (The MathWorks, Natick, MA, USA) (Dubois et al., 2015; Kim et

al., 2018; Taş et al., 2017) and computer aided design (CAD) systems (Gatos et al., 2016, 2017; Xiao et al., 2014). Previously mentioned research groups utilizing MATLAB for processing did not disclose information regarding concatenation of steps compiling the image processing algorithm, possibly for proprietary purposes. However, Gatos et al., 2016 and 2017 and Xiao et al., 2014 utilized the CAD system and briefly provided details regarding their image processing algorithms. Gatos et al., 2016 and 2017 expressed that every pixel within the entire color box, provided by a SWE image, is evaluated and assigned a corresponding stiffness value. Analyzing the entire elastography color box is beneficial when evaluating bigger structures such as the liver for chronic liver disease (Gatos et al., 2016, 2017) and human breasts for tumor (Xiao et al., 2014). However, it would be more beneficial to have the ability to analyze specific areas within the SWE color box; potentially allowing researchers to evaluate smaller structures such as individual muscle fascicles.

Statements of Purpose

1. The primary purpose of this thesis is development and validation of a custom image processing algorithm capable of deducing stiffness values from SWE color boxes produced on the ultrasound machine. Using de-identified ultrasound images of ligament, muscle, and tendon, we will establish reliability and expect to see ICC values of .90 or higher. Following reliability, we will validate our algorithm's stiffness values against those produced on the ultrasound machine.
2. Upon validating our code, the secondary purpose of this thesis is the application of the algorithm. Using a preexisting dataset, we will evaluate muscle stiffness changes occurring in elite track & field athletes during a competitive season. Implementing an outlier analysis, we hope to identify muscle stiffness anomalies; these anomalies may

provide insight into how muscle material properties change due to accumulation of muscular strain and/or muscular injury.

Hypotheses

1. We hypothesize male athletes will have stiffer hamstring muscles overall, when compared to female athlete counterparts.
2. We hypothesize athletes with a history of HSIs will display higher stiffness values than those athletes with no previous HSI history.
3. We hypothesize tracking mean hamstring muscle stiffness in track & field sprinters and jumpers across measurement days will allow us to quantify muscle material property changes among individual athletes.

Significance

Hamstring strain injuries are one of the most common injury types across the globe in elite competition. A three year injury surveillance at the Penn Relays concluded hamstring strains accounted for 24% of all injuries reported (D. A. Opar et al., 2014). Despite reported modifiable risk factors and preventative and rehabilitative programs, hamstring strain incidence continues to increase. Development of techniques that provide accurate assessment of musculoskeletal tissue property deviations will help clinicians determine potential initial injury, treatment and rehabilitation progressions and durations, and return to play for athletes.

Typically, research labs are equipped with one ultrasound machine that is occupied by multiple studies. As a result, shear wave elastography (SWE) image processing is completed solely on the ultrasound machine. A custom processing code will provide clinicians and researchers the ability to assess patients and participants on the ultrasound machine and simultaneously process images away from the machine on a computer. Thus, maximizing the

number of athletes that can be assessed while not monopolizing the ultrasound for image processing, ultimately allowing for more efficient use of the ultrasound machine.

SWE has shown success in its ability to quantify muscle stiffness (Seymore et al., 2017). Like Seymore et al., 2017, previous literature utilizing an ultrasound machine to examine muscle stiffness, uses the machine's built-in software to analyze the shear modulus and assign stiffness values to a given region of interest. Although using the ultrasound machine's built-in software for processing is typical, that software is limited in its capabilities. The built-in software on the ultrasound machine allows the user to either draw a circular region of interest or the user can trace (using a finger or computer stylus) a desired shape. However, for some smaller soft tissue structures a circular shape may not be the best option to define a region of interest and a user traced shape may prove un-reliable. Our custom image processing algorithm will provide the user with the flexibility to determine the best shape to define a region of interest, e.g. a rectangle for large musculature.

This thesis aims to provide more evidence establishing validity and reliability in a custom image processing algorithm's ability to analyze SWE images. The application of this custom code will track shifts in muscle stiffness in healthy at-risk populations, e.g. track & field sprinters, jumpers, and hurdlers. These findings will theoretically provide more insight into the techniques needed to assess muscle stiffness using shear wave elastography, so future healthcare professionals can better determine athletes at increased risk of musculoskeletal injuries.

Delimitations

1. Validation of our custom image processing algorithm will only include muscle, tendon, and ligament soft tissue structures.
2. Subjects are over 18 years of age.

3. Subjects are healthy elite track & field sprinters and jumpers.
4. Previous injury will not exclude volunteers from participating in the study.
5. The study only measures elastography of the left and right hamstring muscles.

Limitations

1. Our custom image processing algorithm will use rectangles, instead of circles like the Supersonic Aixplorer ultrasound machine, when defining a ROI.
2. Small sample size of volunteers.
3. Hamstring stiffness measurements may possibly be altered because of in-season resistance training.

Chapter II. Review of Literature

Introduction

This thesis aims to demonstrate the validity of a custom MATLAB image processing algorithm and establish reliability in tracking shifts in muscle material property changes in a competitive season in elite track & field athletes (preexisting data set). The focus of this literature review will be to exhibit the prevalence of hamstring strain injuries and the burden that ensues after initial and re-injury. Explore the biomechanics of sprinting and injury pathology associated with HSIs. Determine the effects eccentric exercise-based intervention programs can have on hamstring strain injuries. Lastly, this literature review will investigate the history of musculoskeletal elastography imaging; hoping to delineate the most effective and efficient imaging technique for assessment of hamstring strain injury pathology.

Prevalence of Hamstring Strain Injury

Among elite athletes, branching many different sports, the lower limbs appear to be the most susceptible area for injury during trainings and competitions; accounting for almost 54% of all reported injuries in 15 different sports (Hootman et al., 2007). Perhaps, the most common diagnosis within lower limb injuries affect the musculoskeletal system, hamstring strains being the most common injury type (Alonso et al., 2009, 2010, 2012; Crema et al., 2018; Edouard et al., 2016). Over a period of 6 seasons, Major and Minor League Baseball observed a total of 49,995 injuries, hamstring strains being the most common diagnosis, accounting for 6.7% of all injuries (Camp et al., 2018). Within the National Football League (NFL) musculotendinous strains have accounted for 50% of all injuries, hamstring strains being the most common injury type; these injuries averaged 8 days missed per injury incidence (Feeley et al., 2008). In the Australian Football League (AFL) hamstring strain injuries (HSIs) were responsible for an

average of 6 new injuries per club per season (Gabbe et al., 2005; J. Orchard & Seward, 2002; J. W. Orchard et al., 2013). The prevalence of HSIs persists within professional soccer, these injuries compile between 12-37% of all reported injuries (Ekstrand et al., 2011; Fitzharris et al., 2017; Woods et al., 2004). During elite track & field competition, HSIs were the most common diagnosis, ranging between 13.8-24% of all reported injuries and as high as almost 40% of all reported musculoskeletal injuries (Alonso et al., 2009, 2010, 2012; Edouard et al., 2016; D. A. Opar et al., 2014).

Despite new research literature introducing new training protocols to help protect against posterior thigh strains, HSI incidence continues to increase annually (Ekstrand, Waldén, et al., 2016; J. W. Orchard et al., 2013). More alarming, several months after initial return to play athletes appear to be re-injuring the same muscle; at least 13% of all HSIs were similar recurrences, occurring 2 months into return to play (Ekstrand, Waldén, et al., 2016). A Two decade injury surveillance observing the AFL, recorded HSIs to have an average recurrence rate of 26%, causing approximately 20 missed matches per club per season (J. Orchard & Seward, 2002; J. W. Orchard et al., 2013). This recurrence rate is similar to previously reported literature, stating hamstring muscles have a recurrent injury rate between 30-34% (Ekstrand et al., 2011; J. Orchard & Best, 2002; J. Orchard & Seward, 2002; Woods et al., 2004).

Increased re-injury of HSIs are affecting the amount of time athletes are away from trainings and competitions. Time-loss injuries accounted for almost 56% of all injuries during the IAAF World Athletics Championships; at 30.5% of all injuries, hamstring strains were the most common time-loss injury (Alonso et al., 2009).

Recurrent injuries lead to 30% longer absences than non-recurrent injuries, ultimately having severe financial consequences (Ekstrand et al., 2011). Yearly costs for overall

management, rehabilitation, and training for HSIs has increased by 71% from 2003-2012 (Hickey et al., 2014). An approximate time-loss duration of only 14 days from a HSI, can have an average cost as high as 250,000 euros for professional European Football (Ekstrand, Waldén, et al., 2016). A decade long injury surveillance, conducted by the NFL, concluded that HSIs potentially cost a single team an annual average of \$353,469 (Elliott et al., 2011).

Men appear to suffer more HSIs than women, an injury surveillance of elite track & field athletes reported 47.2 vs 32.3 injuries/1000 athletes affecting the thigh region (Alonso et al., 2010). The majority of research literature concludes that men have more HSIs/1000 athletes than women (D. A. Opar et al., 2014). Interestingly, another study reporting on injuries to elite track & field competitors from 2007-2015, found equal proportions of HSIs among male and female athletes, even though they determined men to have higher risk (Edouard et al., 2016). Increased risk for males may be explained by stiffer muscles, measured by standardized joint perturbation loading, and longer muscle fiber lengths within the hamstring muscle complex; this indicates males may be more resistive to muscular length changes, overall increasing risk of strain injury (Blackburn et al., 2009).

Hamstring Strain Injury Mechanisms

High speed running and sprinting consists of four primary gait segments: ipsilateral toe-off, contralateral foot-strike, contralateral toe-off, and ipsilateral foot-strike (Schache et al., 2012). The period between each individual foot-strike and corresponding toe-off is considered “stance phase” and the period following toe-off and the next corresponding foot-strike is considered “swing phase” (Schache et al., 2010, 2012). Determining the exact physiological and biomechanical mechanisms that may lead to a musculoskeletal injury have not been universally established, despite increasing amounts of literature researching injury risk factors.

It is plausible that the mechanism leading to an HSI are a combination of modifiable and non-modifiable risk factors and the kinematics associated with specific bodily movements. For example, dancers frequently perform movements that extremely flex the hip while completely straightening the knee, passively stretching the hamstring muscle (Askling et al., 2007b). This study reported dancers suffering a HSI had considerably longer rehabilitation times, when compared to sprinters suffering a HSI (Askling et al., 2007b; Hincapié et al., 2008). Despite this, literature concludes most HSIs occur from high speed running and sprinting. Injury pathology research associated with sprinting movements conclude these HSIs occur during “terminal swing phase” of the sprinting gait cycle (Heiderscheit et al., 2005; Schache et al., 2009, 2012; Thelen, Chumanov, Hoerth, et al., 2005).

Terminal swing phase is approximately between 60-75% of the sprinting gait cycle (Schache et al., 2012). During sprinting the hamstrings concentrically contract as hip extension occurs, eccentrically contract to decelerate extension of the knee while also stabilizing the knee, and perform a rapid countermovement from knee extension to knee flexion (Clark, 2008; Schache et al., 2010, 2012).

Dissimilar research argues that HSIs may occur by other mechanisms other than acute injury (Zemper, 2005). Research suggests during eccentric contraction muscular injury is caused by accumulation of active muscle strain within muscle (overuse injury), rather than a result of force (acute injury) (Lieber & Fridén, 1993). Modeling of the sprinting gait cycle suggests sprinting and explosive running movements cause the hamstring muscle complex to produce and be placed under large amounts of load (force, power, and negative work) (Schache et al., 2012; Thelen, Chumanov, Best, et al., 2005). However, despite muscles being exposed to large amounts of force causing excessive stretch, 60% beyond resting length, revealed that force was

not the cause of muscle damage (S. V. Brooks et al., 1995). It was determined that eccentrically loaded muscle injury is attributable to a large stretch and not the amount of external force (S. V. Brooks et al., 1995).

Comparably, Lieber & Friden, 1993, measured contractile properties of lower limb rabbit muscles, stretching tibialis anterior muscles to 25% and 12.5% of muscle fiber length at identical lengths. “However, because the timing of the imposed length change relative to muscle activation was different, the groups experienced dramatically different muscle forces” (Lieber & Fridén, 1993). After 30 minutes of cyclic activity muscle maximum tetanic tension and other contractile properties were assessed and found to be identical, regardless of strain timing pattern (Lieber & Fridén, 1993). This study concluded the amount of damage sustained from cyclic eccentric loading was the same despite different imposing forces on the muscles. Two-way ANOVA analysis of experimental strain vs. timing (early vs. late stretch) revealed a substantial effect of muscular strain magnitude ($P < 0.001$) (Lieber & Fridén, 1993). Essentially, muscle damage is not a result of large forces imposed on the muscle, but more a function of accumulated muscular strain magnitude.

The concept of acute hamstring injury theoretically suggests athletes are surpassing the biomechanical and physiological limits within the hamstring muscle complex during every sprinting or high-speed running exposure. This idea is unlikely and not consistently supported by literature. Accumulating muscular strain magnitude appear to be a product of non-uniform lengthening of sarcomeres; resulting in sarcomere length inefficiencies and increased active strain in muscle fibers from repetitive eccentric loading (Lieber & Fridén, 1993; Morgan, 1990). Similarly, eccentric stretch of muscles can cause energy absorption inefficiencies and structural defects (weak points) within muscle fibers (Noonan et al., 1994). Therefore, instead of large

force magnitudes, it is the development of skeletal muscle weak points, due to accumulated microscopic strain damage, that act as the origin of larger and more debilitating musculoskeletal strains (C. L. Brockett et al., 2001; Camilla L. Brockett et al., 2004; Proske & Morgan, 2001).

Ultimately, recurrent performance of eccentric loading with multiple developing areas of microscopic damage, that are undetected by sports medicine personnel, lead to sarcomere length instability (C. L. Brockett et al., 2001; Camilla L. Brockett et al., 2004; Clark, 2008; Morgan, 1990). This evidence suggests why athletes involved in sprinting sports, explosive running activities, and long periods of uninterrupted bouts of repetitive eccentric loading of the hamstrings, are the most at-risk population for sustaining a HSI (Dalton et al., 2015; Edouard et al., 2014; Elliott et al., 2011; Malliaropoulos et al., 2010; David A. Opar et al., 2012; J. W. Orchard et al., 2013; Verrall et al., 2003; Watson & DiMartino, 1987).

Research suggests there are individual differences between the three hamstring muscles, each have varying rates of injury (Askling et al., 2007a; Crema et al., 2018; Heiderscheit et al., 2005; Koulouris et al., 2007; Koulouris & Connell, 2003; Verrall et al., 2003). Biceps femoris is injured the most of the three muscles, involved with 80% of all injuries to the hamstring group (Koulouris et al., 2007; Koulouris & Connell, 2003; Thelen, Chumanov, Best, et al., 2005; Verrall et al., 2003). This may be due in part to greater increases in peak musculotendinous length, 12.2% beyond normal measures compared with 9.8% and 10.4% for semitendinosus and semimembranosus, respectively (Heiderscheit et al., 2005; Schache et al., 2012).

Eccentric Contraction and Exercise Effect on the Hamstring Muscle Complex

Aforementioned evidence reiterates that accumulated active muscle strain is the mechanism that causes a HSI and repetitive eccentric loading occurring in sprinting activities increases injury risk (C. L. Brockett et al., 2004; Garrett, 1990). Eccentric intervention programs

lead to two changes in skeletal muscle. During eccentric exercises, sarcomeres stretch beyond thick and thin filament overlap and remain disrupted after returning to a relaxed state (C. L. Brockett et al., 2001; S. V. Brooks et al., 1995; Susan V. Brooks & Faulkner, 1996). Non-uniform stretching of sarcomeres beyond optimum length, during the descending limb of muscle's length-tension curve, becomes the origin site of muscle fiber disruption (Morgan, 1990; Wood et al., 1993). These initial changes, as described above, are considered to be delayed onset muscle soreness (DOMS); causing small areas of microscopic damage, however temporary, lasting on average 2-3 days post exercise (C. L. Brockett et al., 2001).

A more prolonged change to eccentric exercise has shown transient changes that lead to sarcomerogenesis (increased muscle fiber length), allowing a lasting shift in muscle optimum length, producing a residual training effect in muscle (C. L. Brockett et al., 2001, 2004; Susan V. Brooks & Faulkner, 1996; Lynn & Morgan, 1994; Morgan, 1990; Warren et al., 1993; Wood et al., 1993). Animal studies suggest the observed training effect is a direct result of an increased number of sarcomeres within muscle fibers (Jones et al., 1997; Lynn et al., 1998; Lynn & Morgan, 1994; Morgan, 1990; Wood et al., 1993).

Increased sarcomere numbers (also characterized by increased muscle volume and physiological cross sectional area) due to eccentric interventions may allow hamstring muscle complex to operate at longer lengths while avoiding the region of instability for sarcomere length distributions (C. L. Brockett et al., 2001). Seymore et al., 2017 hypothesized the mechanism behind nordic hamstring curl reducing hamstring injury risk was potentially due to an increase in muscle volume, not fascicle length (Seymore et al., 2017). Two separate articles reporting torque-angle curves for hamstring muscles showed an average shift of 4 degrees and 7.7 degrees, respectively (C. L. Brockett et al., 2001; Seymore et al., 2017). According to Brockett et al.,

2001, larger mean shifts may be a result of not standardizing a fixed hip angle while performing Nordic hamstring (NH) curl, an established eccentric loading intervention exercise.

Standardizing hip angles at 0 degrees may explain the smaller shift in torque-angle curve during NH curl (Seymore et al., 2017). Fixed hip angles during NH curl causes the knee to move through a smaller range of motion, also decreasing possible compensation of hip musculature and increasing active tension placed on hamstring muscles.

Eccentric intervention programs have shown success in decreasing susceptibility to damage and lowering risk of HSIs (Arnason et al., 2008; Petersen et al., 2011; Verrall et al., 2005; Whitehead et al., 1998). Combining NH curl, sport specific agility training, and hip extension exercises has produced evidence of reducing hamstring strain injury incidence, per athletic season, in collegiate track & field sprinters from 137.9 to 6.7 over 24 years (Sugiura et al., 2017).

Musculoskeletal Elastography Imaging

Increasing rates of HSI occurrence, HSI re-injury, and soaring financial costs associated with HSI suggest coaches and sports medicine physicians and clinicians must reevaluate injury prevention models, clinical diagnostic tools, and injury rehabilitation. Researchers should focus on preemptive assessment of muscle material property alterations, allowing for tracking of soft tissue changes prior to injury.

Previously, magnetic resonance imaging (MRI) has proven reliable in assessing frequency of injury location within the musculotendinous unit of the hamstring muscle complex (De Smet & Best, 2000). More recently, magnetic resonance elastography (MRE) has become a popular approach to measure material properties of muscle using MRI technology (Basford et al., 2002; Greenleaf et al., 2003; Suga et al., 2001). MRE uses MRI technology to map and quantify

muscle tissue deformations induced by a cyclical external vibrator (Dresner et al., 2001; Muthupillai et al., 1995). Reliability has been established in assessing muscle stiffness and deep musculature; however, scans can only be performed with a patient supine and equipment procurement cost remains a limiting factor.

Ultrasonography is an essential musculoskeletal imaging tool and with the recent addition of ultrasound elastography, assessment of soft tissue stiffness has grown in the literature (Winn et al., 2016). The term elastography was first introduced into the literature by (J Ophir et al., 1991); this study attempted to describe a new method for quantifying strain and elastic modulus of biological soft tissues. Ophir's method utilized external tissue compression, applying a stress to the targeted soft tissue, and then measures shifts using the ultrasound (J Ophir et al., 1991). Using bacon slabs as the biological soft tissue, Ophir et al., 1991 was able to distinguish between muscle layers and the softer layered fat structures, which were reported to have varying compliance. Elastography is described as a method of quantifying the strain properties of soft tissue (Jonathan Ophir et al., 2002). Elastic modulus of biological tissue suggests how it may respond to an applied strain or stress and is represented by either Young's modulus or shear modulus (Winn et al., 2016).

Currently in the literature, two primary methods of ultrasound elastography are employed in clinical diagnostics. First, the method developed in 1991 by Ophir et al., modernly known as compression/strain elastography, is based on a manually applied force (i.e. from the hands or from the transducer probe) that repetitively compresses soft tissue and tracks displacement (J Ophir et al., 1991; Yanagisawa et al., 2011). Strain elastography is limited by the sonographer's inability to consistently reproduce manually applied force and uncertainties of varying dissipation within skin and subcutaneous fat (Winn et al., 2016; Yoshitake et al., 2014). Second

and more related to this thesis, shear wave elastography (SWE) produces shear waves from ultrasonic focused pulses to generate mechanical vibration sources internally, instead of externally as described by strain elastography (Jonathan Ophir et al., 2002) and MRE (Bercoff et al., 2004; Sarvazyan et al., 1998). SWE is independent of tissue compression and linked displacement, unlike compression/strain elastography, ultimately yielding more reliable measurements (Andonian et al., 2016). SWE evaluates shear wave propagation velocities, then uses those velocities to estimate shear modulus of relaxed or contracted muscle; collected data is then used to quantitatively define stiffness in kilopascals (kPa) (Andonian et al., 2016; Shinohara et al., 2010).

Ultrasound elastography techniques may also prove themselves useful in quickly and reliably assessing mechanical properties of musculoskeletal systems. A study completed by Lacourpaille et al., 2012 took 30 healthy adults and randomly assigned them to three groups, intra-session reliability, inter-day reliability and/or inter-observer reliability. Assessment of intra-session reliability was completed by the same experimenter with a 15 minute rest between same day measurement sessions, inter-day reliability was assessed by the same experimenter on two separate days, and inter-observer reliability was assessed by two separate experimenters with a 15 minute rest between same day measurement sessions (Lacourpaille et al., 2012). The experiment measured nine different muscles with different architecture and fiber type to evaluate the reproducibility and feasibility of ultrasound elastography measurement. Overall, each assessment lasted approximately 20 minutes. Reliability results reported intra-class correlation values of 0.872, 0.815, and 0.709 obtained from the three different experimental groups, respectively (Lacourpaille et al., 2012). With established reproducibility and feasibility, ultrasound elastography seems a viable assessment tool of healthy muscle in vivo. However,

more research needs to be collected to determine if ultrasound elastography can be used as tool to determine muscle injury pathologies.

Exploring and validating the quantitative assessment capabilities of SWE to track changes in skeletal muscle properties is a promising topic for future research, as it may be useful in improving injury prevention strategies and identifying muscular injury pathologies (Andonian et al., 2016). Andonian et al., 2016 may be the first article that monitored muscle stiffness changes pre, during, and post prolonged mechanical loading from an extreme mountain ultra-marathon, observing a decreasing trend in quadriceps muscle stiffness. More recently, tracking changes in muscle shear wave speed of distance runners using SWE demonstrated running distance had an effect on biceps femoris and semitendinosus muscle ($p = 0.02$) (Sadeghi, Newman, et al., 2018). Briefly, the study found semitendinosus shear wave speed decreased one day after competition in short (3-5 miles), medium (10-13 miles), and long (26+ miles) running groups and biceps femoris decreased after one day in the medium group. Similarly within ligaments, SWE has shown positive capabilities in tracking shear modulus in overhead throwing athletes (baseball pitchers and football quarterbacks) over a 14-week competitive season (Sadeghi, Lin, et al., 2018). Monitoring changes in shear modulus throughout a competitive season may be of interest for sports medicine physicians, coaches, and other clinicians in an effort to improve training and intervention protocols prior to injury (Sadeghi, Lin, et al., 2018).

When interpreting SWE mean stiffness calculations it is important to be mindful of how these values were processed. Typically, most ultrasound machines have a built-in tool that allows for direct processing of collected images on the machine. In recently published literature, research groups have opted to process SWE images away from the ultrasound machine using a custom code. In a 2014 study by Xiao et al., a computer-aided design (CAD) was developed to

improve diagnostic accuracy of classification of breast tumors, in hopes of avoiding unnecessary biopsies. Similarly, in 2016 Gatos et al., adopted a comparable CAD inverse mapping technique in hopes of improving diagnostic accuracy of chronic liver disease and as a tool to aid in avoiding needless biopsies. It seems other research groups have also employed MATLAB (The MathWorks, Natick, MA, USA) software to develop their own image processing algorithms, but they did not reveal specifics of their image processing algorithm's stepwise progressions (Dubois et al., 2015; Kim et al., 2018; Taş et al., 2017). The three studies using MATLAB algorithms to process data each reported that SWE is a reliable method in evaluating shear modulus; however, none of them provided validity testing results for their custom image processing algorithm. Producing validity results is important in interpreting whether the stiffness values produced from the algorithm match those stiffness values produced by the ultrasound machine. Conversely, Gatos et al., 2016 provided validity results for their CAD inverse mapping algorithm. This research group concluded that their programmatically produced stiffness values had an average difference of 0.01 ± 0.001 kPa when compared with values produced by the Aixplorer ultrasound machine's built-in Q-box tool.

From the current review, SWE seems to be an appropriate tool for assessment of muscle shear modulus, demonstrating strong reliability and reproducibility (Dubois et al., 2015). Utilizing SWE to monitor changes in muscle shear modulus has potential to be a viable clinical tool in assessment of muscle prior to injury, throughout the rehabilitative regimen, and recovery. However, more research is needed; specifically, research validating processing techniques and research establishing reliable capabilities of hamstring muscle stiffness tracking. Future examination into these areas may help in determining if hamstring muscle strain injury pathology can be identified via SWE.

Summary

In summary, increasing incidence of hamstring strains and elevated risks for re-injury are causing athletes to miss more time from trainings and competitions. Muscular strain injuries in elite athletics are inevitable, but a better understanding of injury mechanisms is required if athletes, coaches, and clinicians have a desire to reduce incidence rates. For HSIs it appears that the small areas of disruption that develop from repetitive eccentric loading are the initial sites of strain. These developing weak points within sarcomeres, if untreated, may lead to more severe injury if eccentric loading continues.

Often those initial disrupted fibers within muscle are undetected because they are microscopic in nature and not every athlete, symptomatic or asymptomatic, is regularly assessed by clinicians. MRE is too expensive of a tool for wide clinical use, rendering it difficult to gain access too. Ultrasound B-mode image has shown the ability to detect muscle injury, but it may not detect those microscopic damages. SWE is an emerging technology that has potential to regularly measure microscopic muscle material property changes, however lacking substantial research because of its novelty.

More research providing valid and reliable measurement protocols for assessing muscle stiffness can lead to quick preemptive clinical assessment of athletes with strong reproducibility. The purpose of this thesis is to develop and validate an algorithm capable of processing SWE imaging data. Upon successful validation, we plan on implementing the algorithm to process elastography data from a pre-existing dataset.

Chapter III. Methods

Introduction

This thesis developed a custom image processing algorithm capable of assessing stiffness in SWE images. Development of this algorithm may allow researchers to process SWE imaging data more efficiently away from the ultrasound machine, ultimately creating more availability for the ultrasound machine to collect imaging data. Using de-identified images of different tissue types, we validated stiffness assessments produced from our custom image processing algorithm against stiffness values produced on the ultrasound machine.

Upon validating of the algorithm, we applied it to an available small dataset. This pre-existing dataset was removed from the ultrasound machine prior to being fully processed; therefore, used our custom image processing algorithm to process this imaging dataset completely. The pre-existing dataset utilized SWE to quantify changes in collegiate track & field sprinters', jumpers', and hurdlers' muscle shear modulus. Muscle shear modulus was initially measured at the beginning of the competitive season and subsequent identical monthly data collections were administered. If an athlete indicated they had suffered an HSI, they were asked to return for measurement as soon as possible and the sonographer documented all preceding activities associated with the injury. All procedures were approved by the University Internal Review Board.

Exclusion Criteria

1. Track & field athletes not participating in these events: 100 meters, 200 meters, 400 meters, 4x100 meter relay, 4x200 meter relay, 4x400 meter relay, 100/110-meter hurdles, 400-meter hurdles, long jump, and triple jump.

2. Below the age of 18.

Participants

All participants were volunteers from the East Carolina University track & field team, competing either as a sprinter, jumper, or hurdler. All participants were above the age of 18 years old. A demographic questionnaire (see Appendix B) was completed by each participant, in addition to an informed consent (see Appendix C). The questionnaire gathered information about previous and/or current history of HSIs and location (right or left leg and proximal, mid-belly, or distal) of previous and/or current HSIs. The specific track & field events each athlete participated in and if applicable, leg dominance, start leg (sprinters), lead leg and trail leg (hurdlers), and jumping leg (jumpers) were also gathered from the questionnaire. Data gathered from participant questionnaires is displayed in tables 1 and 2.

Table 1: Participant Demographics

	Mean	St. Dev.
Age	19.67	1.41
Height (cm)	175.77	8.41
Weight (kg)	70.27	10.13

Table 2: Participant Injury History and Events Competed in

Subject #	Sex	Events	Current Injury	Location	Past Injury	When	Location	Start Leg	Lead Leg	Jumping Leg
S001	M	LS, SS, LH	No	N/A	Yes	3 yrs	Both	Both	Both	N/A
S002	F	SS, LS	No	N/A	Yes	1 yr	Both	Left	N/A	N/A
S003										
S004	M	LS	No	N/A	No	N/A	N/A	Right	N/A	N/A
S005	M	LS, SH, LH	No	N/A	Yes	9 mos	RP	Both	Left	Left
S006	F	SS, LS, LJ	No	N/A	Yes	7 mos, 2 yrs	LD, RM	Left	Right	Right
S007	M		No	N/A	No	N/A	N/A	Right	Left	Right
S008	M	SH, LH	No	N/A	Yes	4 mos	LP	Right	Left	Left
S009	M	LS	Yes	R	No	N/A	N/A	Left	N/A	N/A
S010	F	SH, PV	No	N/A	No	N/A	N/A	Right	Left	Both
S011	F	Multis	No	N/A	No	N/A	N/A	Right	Right	Left
S012	F	SS, LS	No	N/A	Yes	2 yrs	R	Right	N/A	N/A
S013	F	SS, LS	No	N/A	No	N/A	N/A	Left	N/A	N/A
S014										
S015	F	LH, Multis	No	N/A	Yes	9 mos	RD	Right	Right	Left

Events:

SS = short sprint (60m, 100m)
 LS = long sprint (200m, 400m)
 SH = short hurdle (55/60m H, 100/110m H)
 LH = 400m H
 LJ = long jump
 TJ = triple jump
 HJ = high jump
 Multis = heptathlon, decathlon

Location

R = right hamstring
 L = left hamstring
 Both = both hamstrings
 P = proximal
 M = mid-belly
 D = distal

Equipment and Instrumentation

Shear wave elastography and B-mode images were taken with a Supersonic Aixplorer (SuperSonic Imagine, S.A., Aix-en-Provence, France). Images were captured using a SuperLinear™ SL15-4 musculoskeletal transducer (SuperSonic Imagine, S.A., Aix-en-Provence, France). To assist in wave propagation, an ultrasound gel was placed on the SL 15-4 transducer during measurements. Height and weight data were documented with a Seca 703 digital scale (Seca gmbn & Co.kg, Hamburg, Germany).

Image processing algorithm was developed using MATLAB 2016a (The MathWorks, Natick, MA, USA). MATLAB is widely used computer programming language in biomechanics research. The use of this software provides the possibility to select analysis areas, independent of the measurement area selected on the ultrasound machine (Taş et al., 2017). MATLAB also

features a variety of built-in custom functions in their image processing toolbox, whereas other programming languages do not.

Measurement Protocol

The information below describes in detail the protocols used to collect the preexisting data set. This includes, documentation signed by each participant, participant specific measures, ultrasound collection setup, and actual data collection phases.

Prior to shear wave elastography an informed consent was given to participants for them to read and sign. Participants' height and weight were also recorded. Once the questionnaire was completed, participants lay prone on the training table for shear wave elastography assessment.

The range of stiffness values during SWE assessment was fixed from 0-100 kPa (*figure 1*). Soft tissue structures that are stiffer are displayed red, while less-stiff structures are displayed blue. Every SWE image was also collected at 50% opacity, default setting for the Supersonic Aixplorer. The ultrasound probe was oriented parallel to the muscle during stiffness readings, allowing for better shear wave propagation.

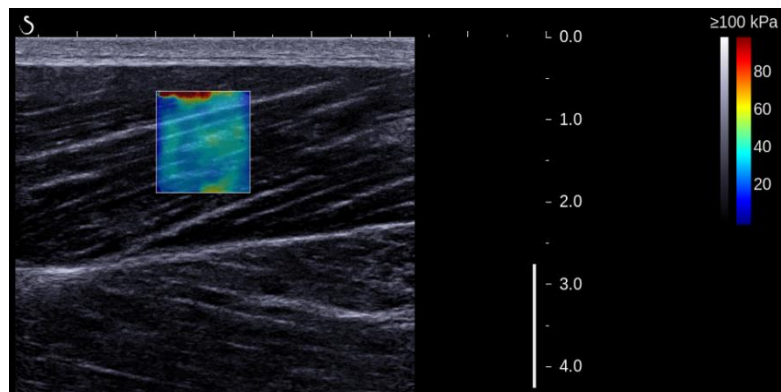


Figure 1: Displays rgb range within a SWE elastogram

Despite the described user selected settings for stiffness range and image opacity from the preexisting data set, our MATLAB processing algorithm will have the capacity to assess images of all opacity scales and measure structures below or beyond 100 kPa.

Measurement protocol evaluated right and left biceps femoris, semitendinosus, and semimembranosus in three different regions (proximal, mid-belly, and distal). A minimum of three elastography measurements were taken at each site, totaling at least fifty-four images per participant per session. Participants were asked to return once per month for the duration of the athlete's training and competitive season to repeat the day 1 measurement protocol. To standardize measurements of muscles in every region between days, distances were marked and measured from the lateral knee epicondyle to the probe position. Athletes suffering an injury, in training or competition, were asked to recall where on the posterior thigh the injury occurred and to describe the events preceding injury occurrence.

Data Processing

Based on literature, processing of SWE images is primarily accomplished directly on the ultrasound machine. Using the Q-box tool, stiffness readings are provided by a circle region of interest (ROI). Once the ROI is established, ultrasound machine's software calculates mean, minimum, maximum, and

standard deviation stiffness values for the ROI. The remaining non-processed data, from the preexisting data set, was removed from the ultrasound machine.

Therefore, data processing to determine stiffness from

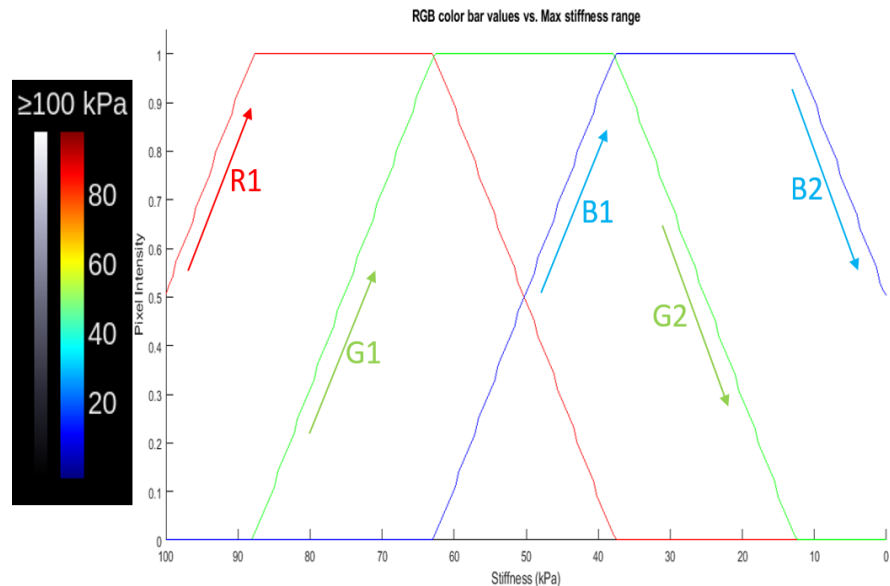


Figure 2: Ascending Segment of Red Color Bar Data (R1), Ascending Segment of Green Color Bar Data (G1), Ascending Segment of Blue Color Bar Data (B1), Descending Segment of Green Color Bar Data (G2), and Descending Segment of Blue Color Bar Data (B2).

the distal, mid-belly, and proximal locations for the hamstring muscle on both left and right legs was completed in MATLAB.

A custom MATLAB algorithm, modeling the output components derived from processed images on the ultrasound machine, was run on every image. Initially, MATLAB command “uigetfile” was called, selecting the image to be analyzed. Calling the built-in MATLAB function “uigetfile” displayed a user interactive box, prompting the user to select a “.png” image for analyzing. Selected image was stored as variable “SWE_image”. The script then programmatically cropped that image’s RGB color bar (upper right corner), storing it as a data variable. Polynomial model line fit equations, MATLAB 2016a built-in function “fit”, were created and individually fitted to ascending and descending segments of each red, green, and blue color bar data vectors (*figure 2*). Output arguments from “fit” function included the polynomial model line fit equation and a MATLAB “struct” containing “Goodness of Fit” statistics. Each line fit equation (R1, G1, B1, G2, and B2) had an r^2 value of 0.9991 or higher, establishing an excellent fit to the inputted data. Each RGB polynomial model line fit equation was implemented to determine stiffness values for all images in this data set.

Secondly, the script accounted for the image opacity settings and then defined a ROI within the selected SWE_image. As mentioned previously, the user selected setting for image opacity was set to

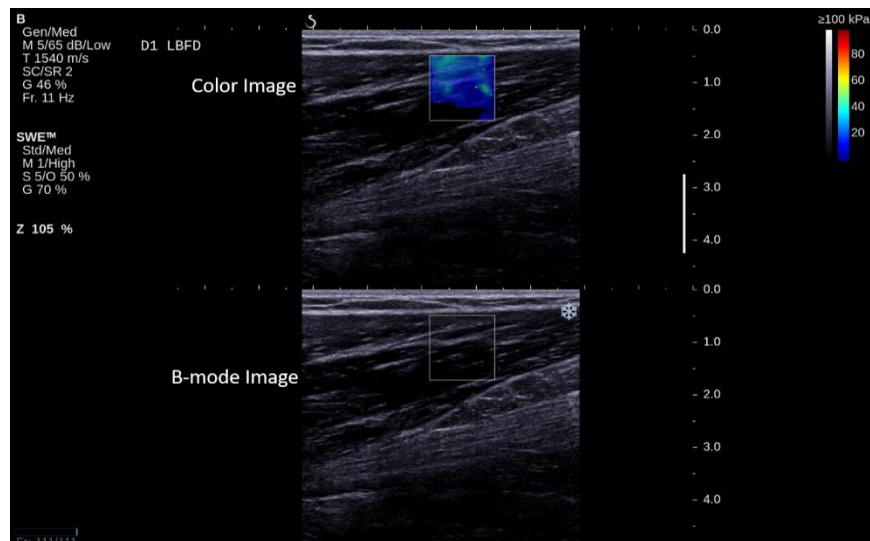


Figure 3: Top Graphic: Shear Modulus Elastogram Superimposed Over B-Mode Image (CI) Bottom Graphic: B-Mode Image (BM)

50%. Assuming the true pixel intensity values located within each elastogram are a weighted average of the top graphic (shear elastic modulus superimposed over b-mode image) and the bottom graphic (b-mode image) as seen in *figure 3*. This relationship is mathematically represented below (*equation 1: a*):

$$\text{a) Color Image} = \frac{\text{Bmode} + \text{True color values}}{2}$$

$$\text{b) True color values} = 2 * \text{Color Image} - \text{Bmode}$$

Equation 1

Table 3: Changes to Pixel Intensity Values After Equation 1 is Applied

"Color Image"	"Bmode"	<i>Equation 1: b</i>	"True Color Values"
0.1059	0.0235	True Color Values = 2*Color Image - Bmode	0.1883
0.1255	0.0235		0.2275
0.1608	0.0235		0.2981
0.1804	0.0235		0.3373
0.2039	0.051		0.3568
0.2314	0.1333		0.3295
0.1804	0.0824		0.2784
0.1922	0.1059		0.2785
0.2314	0.1333		0.3295
0.1765	0.1333		0.2197
0.1882	0.149		0.2274
0.1608	0.1333		0.1883
0.1686	0.1608		0.1764
0.1882	0.1608		0.2156
0.2039	0.2118		0.196
0.2039	0.2118		0.196
0.2196	0.2275		0.2117
0.2471	0.2667		0.2275

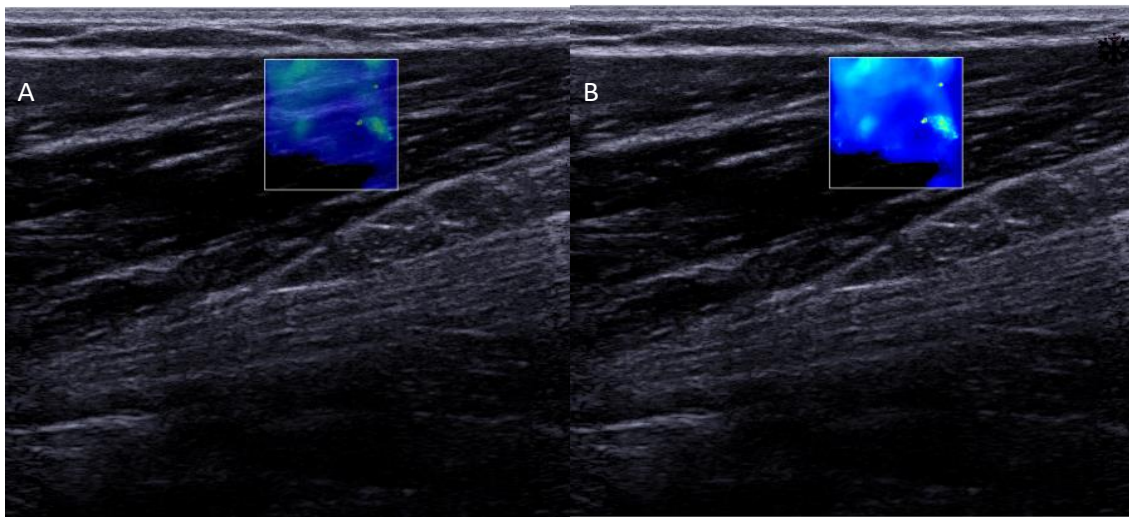


Figure 4: A: SWE_image Before Accounting for 50% Image Opacity Setting. B: Effects of Equation 1 After 50% Image Opacity Setting Has Been Accounted for

Variable “Bmode” represents pixel intensity values located within the B-mode image (*figure 3: bottom graphic*). Pixel intensity values corresponding to the true color map is represented by variable “True color values”. Variables, “Bmode” and “True color values”, are theoretically averaged and the result is represented by “Color Image” (*figure 3: top graphic*). Given our algorithm provides us values for “Color Image” and “Bmode”, we must solve for “True color values”; thus, accounting for the 50% opacity setting and allowing calculation of true pixel intensity values to analyze stiffness. The resulting true color value calculation is expressed in *equation 1: b*. Table 1 provides example pixel intensity values and results after each value is inputted into *equation 1*. Effects from *equation 1* on the image being analyzed is visualized in *figure 4*.

Supersonic Aixplorer ultrasound machine defines its ROI in the shape of a circle. Unfortunately, when programmatically creating a circle ROI we were unable to account for partial pixels that may or may not be included by the ultrasound machine’s calculation a ROI. We propose drawing ROIs in rectangles are easier when working with muscle groups that have a large area and programmatically, we can include any potential partial pixels near the corners of our ROI. Built-in MATLAB function “imrect” was called, allowing the user to click, drag, and release, drawing a rectangular ROI in the center of the elastogram on SWE_image. Positioning of the ROI must begin at the upper left corner, meaning the user must place the cursor there prior to drawing the ROI. To calculate the position of the ROI “getPosition (ROI)” is called; this function’s output argument is displayed in the following syntax: [Xmin Ymin Width Height]. It should be noted that “Xmin” and “Ymin” represent the coordinates of the lower left corner of the ROI. Utilizing this output argument, x and y coordinates of the corners of the ROI can be calculated and stored into X and Y column vectors.

- a) $X = [Xmin; Xmin + Width; Xmin + Width; + Xmin]$
- b) $Y = [Ymin; Ymin; Ymin + Height; Ymin + Height]$

Equation 1

Coordinate vectors X and Y, in combination with image variable produced after 50% opacity setting was accounted for, were used as input arguments for MATLAB function “improfile”. This function used ROI position data to extract every true color pixel intensity value for each RGB color triplet located inside the ROI and stored that data in a matrix.

Prior to establishing stiffness values, each RGB color triplet’s pixel intensity value must be evaluated for valid stiffness information. Pixels not containing valid stiffness information excluded in any stiffness measurement calculations (Gatos et al., 2016). Therefore, all the pixels, calculated from calling “improfile”, must be checked to confirm each pixel contains valid stiffness information. A conditional statement was written stating that if a certain pixel intensity value was below a certain threshold for each RGB color triplet then the algorithm stopped running and provided the user with an error message. If it is determined each pixel contained valid stiffness information, the algorithm printed a message to the MATLAB workspace stating so.

Lastly, the algorithm assigned a stiffness value to each RGB color triplet within the ROI. Recent literature, using MATLAB to assess soft tissue stiffness, converted each RGB color triplet’s pixel intensity values to a single stiffness value according to the values of the color bar (Dubois et al., 2015; Mendes et al., 2018). A for-loop with embedded “if-statements” will iterate through the matrix containing RGB color triplet pixel intensity values. The for-loop evaluated each individual RGB color triplet; depending on each red, green, and blue pixel intensity value the “if-statements” determined which polynomial line fit equation was called to assign a stiffness

value. The end of the loop returns a matrix containing stiffness; mean, median, standard deviation, minimum, and maximum are then calculated and placed into a table. A flowchart outlining specific sequences in algorithm's script can be found in Appendix D.

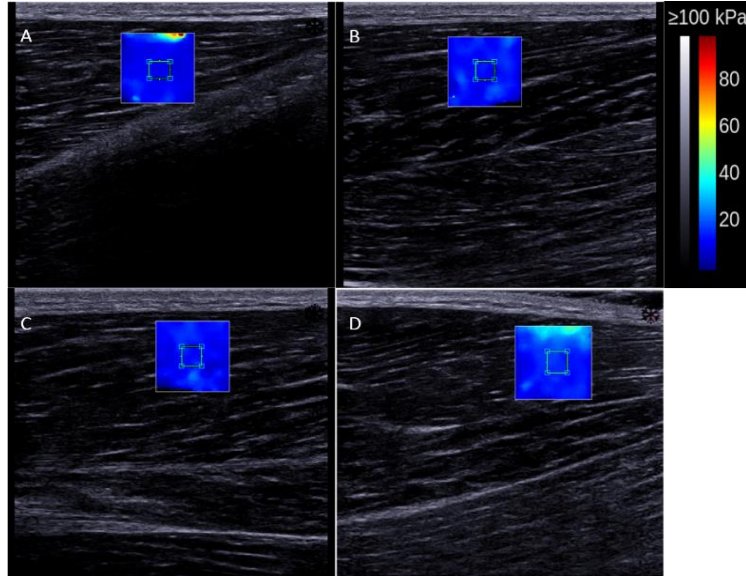


Figure 5: A: Biceps Femoris (BF) Distal 1 B: BF Mid-Belly 1 C: BF Proximal 1 D: BF Distal 2

Pilot Testing of MATLAB Algorithm

Images used in pilot testing had max kPa set to 100, opacity in default setting at 50%, and the orientation of the probe was parallel to muscle. Piloting the algorithm produced a user drawn rectangular ROI in the center of the elastogram (*figure 5*). Stiffness values produced from the algorithm can be seen in *table 4*.

Table 4: Pilot Data Results

	Stiffness (kPa)	Median	Standard Dev.	Minimum	Maximum
A.LBFD 1	11.59	11.74	0.82	9.66	12.72
B.LBFM 1	12.77	12.61	0.84	11.74	15.28
C.LBFP 1	12.63	12.61	0.13	11.85	12.72
D.RBFD 2	15.45	15.38	2.67	12.61	21.18

Statistical Analysis

Reliability Analysis of Custom Image Processing Algorithm

Intraclass correlation coefficient (ICC) analysis of mean values between inter-day sessions will provide information regarding our custom algorithm's reliability in determining stiffness assessments of SWE images. Standard error measurement (SEM) will be calculated to determine inter-day consistency of our custom image processing algorithm. Reliability of this algorithm will be established using de-identified images from other research lab protocols. De-identified images will be selected to include different structures such as muscle, tendon, and ligament.

Validation Analysis of Custom Image Processing Algorithm

Based on the evidence gathered from Zaki et al., 2012, using a Bland-Altman limits of agreement statistical analysis method we aimed to validate our MATLAB algorithm against stiffness means collected directly on the ultrasound machine (considered gold standard). Bland-Altman statistical methodology has shown strong evidence as the best statistical analysis tool when assessing agreement between medical instruments (Zaki et al., 2012). This statistical analysis method is the most widely used method in comparing medical instruments in specialty areas such as medicine, surgery, radiology, and nutrition (Zaki et al., 2012).

Analysis of Pre-existing Dataset

Following validation of the custom SWE image processing algorithm, the previously collected track & field hamstring dataset will be analyzed using our new custom algorithm. With a smaller sample size of 14 participants from the preexisting data set, the ability to run statistical analysis was restricted. We primarily used descriptive statistics to evaluate any potential individual hamstring stiffness differences between genders. We also planned to evaluate

stiffness differences between athletes that have a history of HSI compared to athletes with no previous history of HSI. Cohen's D effect sizes were calculated to evaluate significance of any potential differences between male and female athletes and athletes with a previous HSI history vs. athletes with no previous HSI history. Interpreting the magnitude of each effect sizes, the following scale was used: <0.20 (no effect), 0.20-0.49 (small effect), 0.50-0.79 (medium effect), 0.80-1.29 (large effect), and greater than 1.30 (very large effect) (Rosenthal, 1996).

Most participants (N = 8) completed two days or more of elastography measurements; however, some participants only completed one day of elastography measurements. Due to this fact, our descriptive analysis of gender differences and previous HSI history vs. no previous HSI history included only measurement day one data. Data from measurement day one produced 117 analysis data points for each biceps femoris, semitendinosus, and semimembranosus. On measurement day one, S009 injured their right hamstring muscle; this data point was substituted with S009 day three so that gender differences and previous injury vs. no previous HSI history will not be skewed by this injury data point.

An outlier analysis will be used to evaluate stiffness differences between biceps femoris, semitendinosus, and semimembranosus (147 analysis data points for each muscle, respectively) at each measurement location across measurement days. Only those participants with more than one measurement day of elastography data were included in the outlier analysis. Box plots were created in Microsoft Excel to determine if any outliers exist within individual hamstring muscles. Briefly, boxplots display a 5-number summary of a data set: minimum, 1st quartile (Q1), median, 3rd quartile (Q3), and maximum. Frequently in research outliers produced from an outlier analysis are excluded from further data analysis and interpretation, because it is determined any potential outliers are considered infrequently occurring data points.

Dissimilarly, when analyzing individual participant muscle stiffness values, an outlier can possibly provide insight into the condition of muscle in a distressed state. We postulate any identified outliers may indicate injury or increased risk of potential injury resulting from an accumulation of microscopic damage. An outlier analysis will determine which stiffness changes in individual hamstring muscles are 1.5 times below or above our data's interquartile range (IQR). Outliers are calculated with the following equation:

$$1. \textit{ Lower Range Outlier Limits} = Q1 - (1.5 * IQR)$$

$$2. \textit{ Upper Range Outlier Limits} = Q3 + (1.5 * IQR)$$

Equation 2

Lastly, we used descriptive statistics to analyze mean hamstring stiffness changes throughout the competitive season. We hypothesize any stiffness differences across measurement days greater than our SEM indicate real changes in tissue. Analyzing hamstring stiffness means will allow us to determine how the effects of a competitive season impacted hamstring muscles.

Chapter IV. Results

Reliability of Custom Algorithm

Inter-day reliability for the custom algorithm produced excellent ICC values of 0.999, 0.999, and 0.998 for muscle, tendon, and ligament, respectively. Absolute SEM values, calculated from our reliability results, were 0.01kPa, 0.06kPa, and 0.14kPa for muscle, tendon, and ligament, respectively. Relative SEM, expressed relative to mean difference between day to day reliability assessments, were 4.55%, 16.22%, and 6.8% for muscle, tendon, and ligament, respectively.

Validation of Algorithm Against the Ultrasound Machine

Muscle, tendon, and ligament images were then analyzed using the custom image processing algorithm. To validate our algorithm, stiffness calculations from the algorithm and from the ultrasound machine were compared and analyzed with Bland-Altman plots (*figures 6-8*). Absolute mean differences between both measurement techniques and 95% limits of agreement (LOA) were reported as 0.05 kPa (± 0.77), 3.23 kPa (± 13.35), and 5.32 kPa (± 20.01) for muscle, tendon, and ligament, respectively (*table 5*). When compared to stiffness means from both measurement techniques, we calculated relative stiffness differences of 0.16%, 2.43%, and 1.77% for muscle, tendon, and ligament, respectively (*table 5*).

Table 5: Absolute and Relative Mean Differences Between Algorithm and Ultrasound Machine

Tissue Type	Absolute Mean Differences Between Measurement Techniques (kPa)	Relative Mean Differences Between Measurement Techniques (%)
	Mean \pm LOA _{95%}	Mean \pm LOA _{95%}
Muscle	0.05 \pm 0.77	0.16 \pm 2.43
Tendon	3.23 \pm 13.35	2.43 \pm 10.06
Ligament	5.32 \pm 20.01	1.77 \pm 6.66

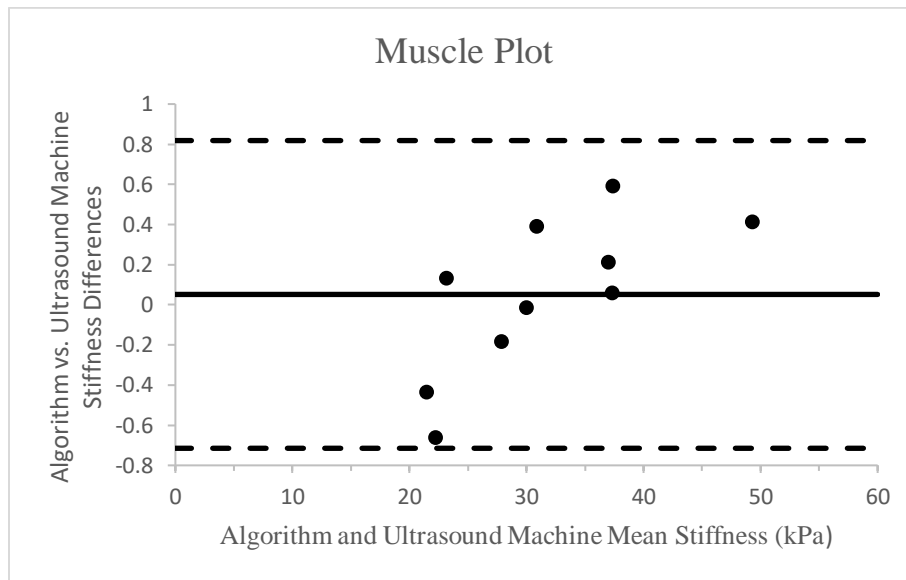


Figure 6: De-identified Muscle Images Bland-Altman Plot

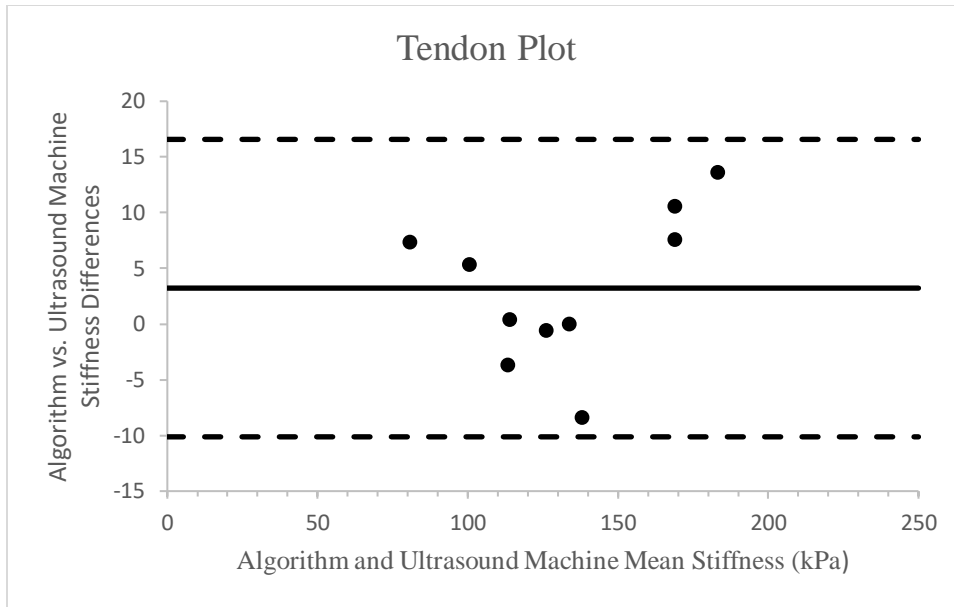


Figure 7: De-identified Tendon Images Bland-Altman Plot

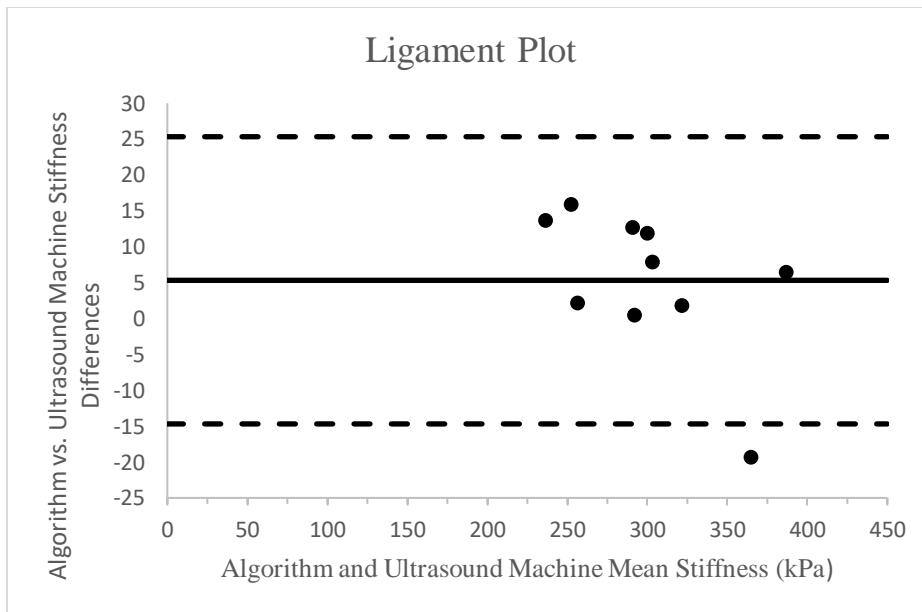


Figure 8: De-identified Ligament Images Bland-Altman Plot

Hamstring Stiffness Gender Differences: Day One Data

S003 and S014 were omitted from this analysis because of missing demographic information and lack of data collection adherence, respectively. A total of thirteen participants

were included in analysis of hamstring stiffness gender differences. Most study participants were female (N = 7), including 46% males (N = 6) (*table 2*). Hamstring muscle stiffness for females averaged 15.24 ± 2.22 kPa, 18.33 ± 4.64 kPa, and 17.55 ± 2.18 kPa for biceps femoris, semitendinosus and semimembranosus, respectively (*figure 9*). Hamstring muscle stiffness for males averaged 15.48 ± 2.34 kPa, 20.07 ± 3.33 kPa, and 18.66 ± 2.64 kPa for biceps femoris, semitendinosus, and semimembranosus, respectively. Gender difference effect sizes were calculated as 0.11, 0.44, and 0.46 for biceps femoris, semitendinosus, and semimembranosus, respectively. Semitendinosus and semimembranosus musculature measured to be 8.67% and 5.95% stiffer in males than in females.

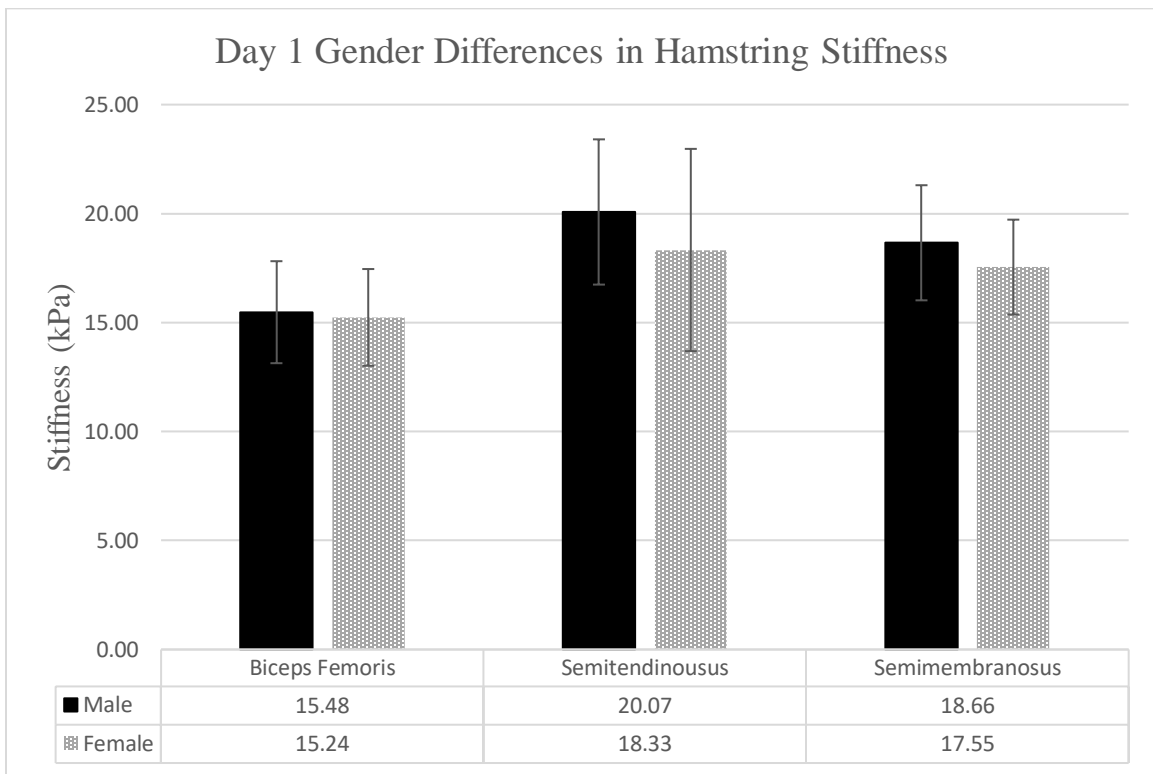


Figure 9: Gender Stiffness Differences within Individual Hamstring Muscles

Previous HSI History vs. No HSI History: Day One Data

Thirteen participants were included in our comparison of stiffness values for athletes with a previous history of HSIs (N = 7) vs. athletes with no previous HSI history (N = 6). S009 was

the only participant reporting a current HSI (Grade I HSI in their right leg, diagnosed by an athletic trainer) (*table 2*). Semimembranosus muscle saw similar stiffness values between comparison groups. Athletes with a history of hamstring strain injury appeared to have less stiff tissue than athletes without a history of HSI in biceps femoris and semitendinosus. Hamstring stiffness for athletes with HSI history averaged 14.41 ± 1.54 kPa, $18.75 \text{ kPa} \pm 4.00$ kPa, and 18.12 ± 2.66 kPa for biceps femoris, semitendinosus, and semimembranosus, respectively (*figure 10*). Hamstring stiffness for athletes with no previous HSI history averaged 16.44 ± 2.43 kPa, 19.59 ± 4.40 kPa, and 17.98 ± 2.23 kPa for biceps femoris, semitendinosus, and semimembranosus, respectively (*figure 10*). Effect sizes were calculated as 1.02, 0.20, and 0.06 for biceps femoris, semitendinosus, and semimembranosus, respectively. Participants with no previous injury history had 12.35% (2.43 SD) and 4.29% (4.39 SD) stiffer biceps femoris and semitendinosus, respectively.

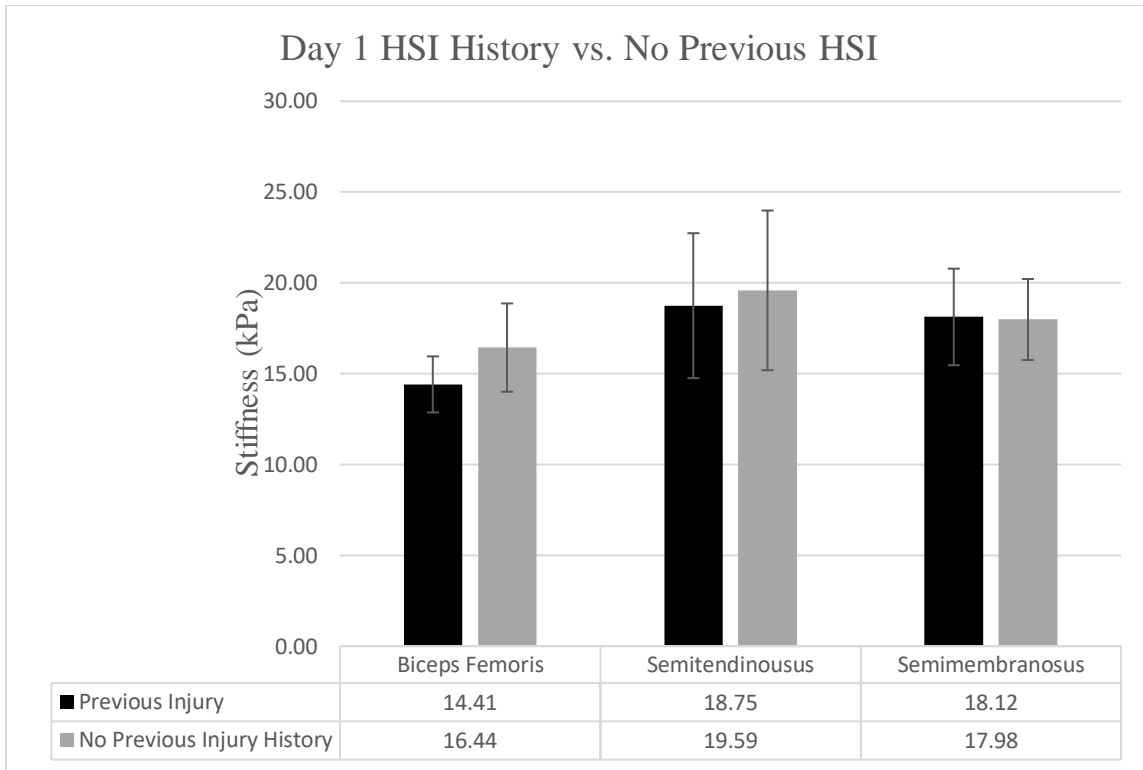


Figure 10: HSI History vs. No HSI History and Its Impact on Muscle Stiffness

Outlier Analysis of Individual Participant Hamstring Stiffness

Our outlier analysis included only those individuals (N = 8) with at least two measurement days' worth of data. Six total outliers were calculated from biceps femoris muscle data (*figure 11*). Five outliers were calculated from semimembranosus data (*figure 13*). Semitendinosus muscle data did not produce any outliers (*figure 12*). Examining individual muscles and comparing stiffness values at each location revealed biceps femoris and semitendinosus proximal muscle stiffness were significantly less stiff than the distal location (*figure 11 and 12*). Figure 13 shows semimembranosus distal location was significantly less stiff than the mid-belly location.

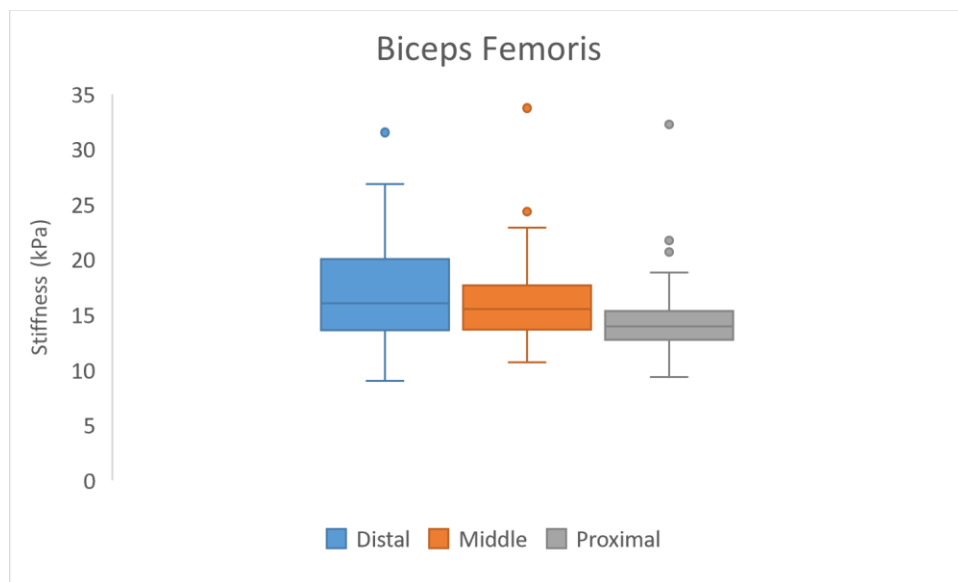


Figure 11: Stiffness Differences in Biceps Femoris Muscle at Separate Locations

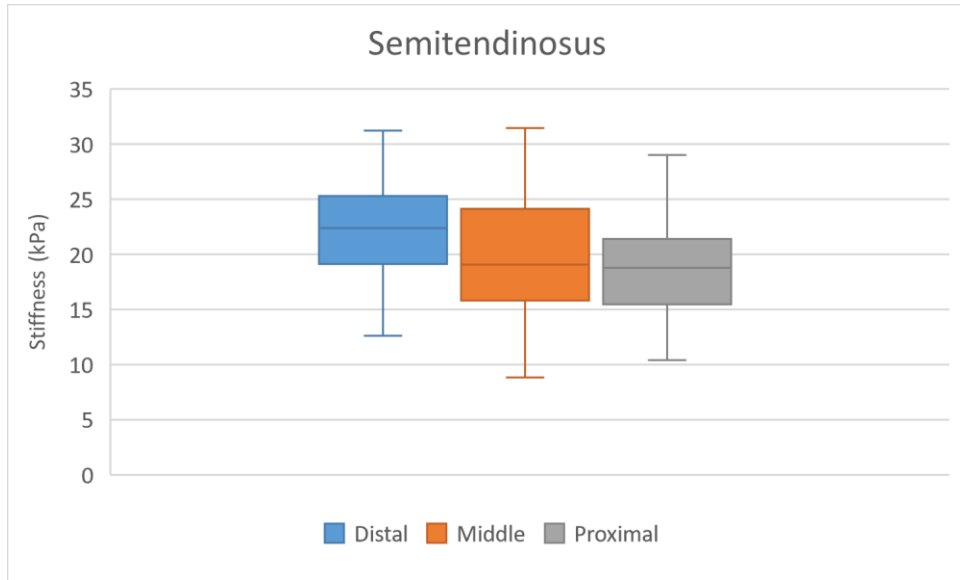


Figure 12: Stiffness Differences in Semitendinosus Muscle at Separate Locations

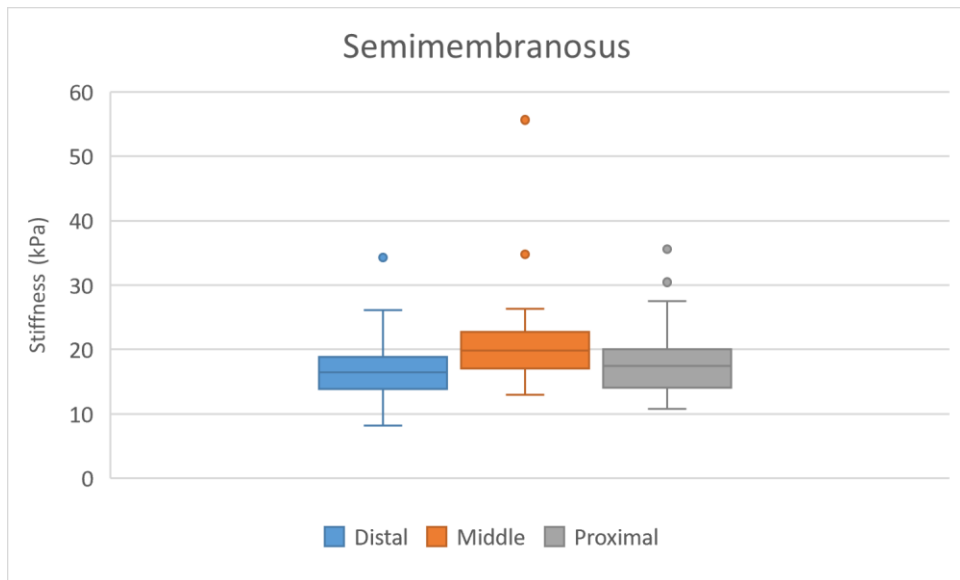


Figure 13: Stiffness Differences in Semimembranosus Muscle at Separate Locations

Tracking Individual Participant Hamstring Stiffness Throughout Competitive Season

Each individual hamstring muscle at each location (distal, mid-belly, and proximal) for both left and right legs were plotted (18 total plots) to track changes occurring in muscle stiffness across measurement days. The analysis included only the participants that had at least two measurement days' worth of elastography data (N = 8). Figure 14 illustrates how most hamstring muscles generally changed throughout a season. Figure 15-17 reveal some participants experienced significant stiffness changes across measurement days. The remaining plots can be viewed in Appendix A.

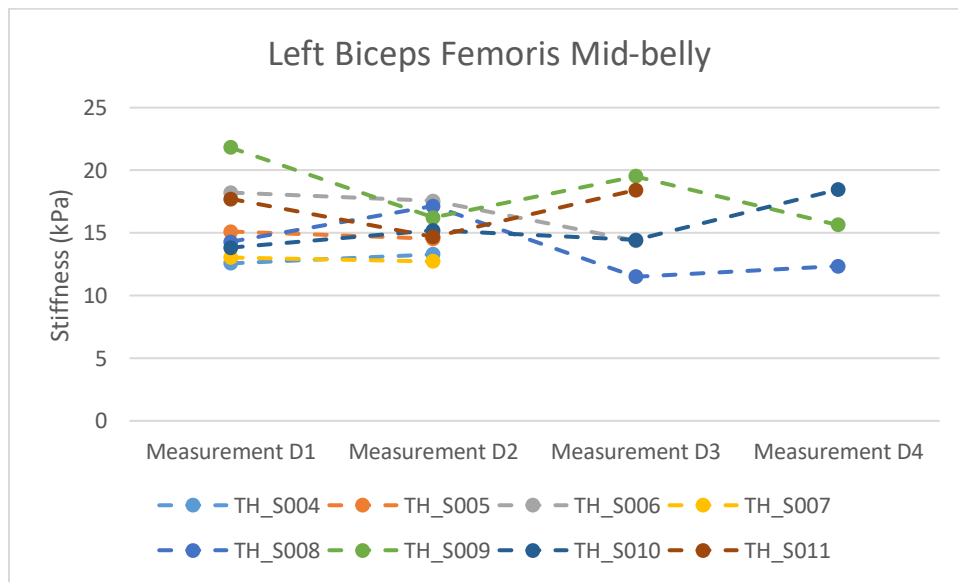


Figure 14: Individual Participant Left Biceps Femoris Mid-Belly Stiffness Changes Throughout Competitive Season

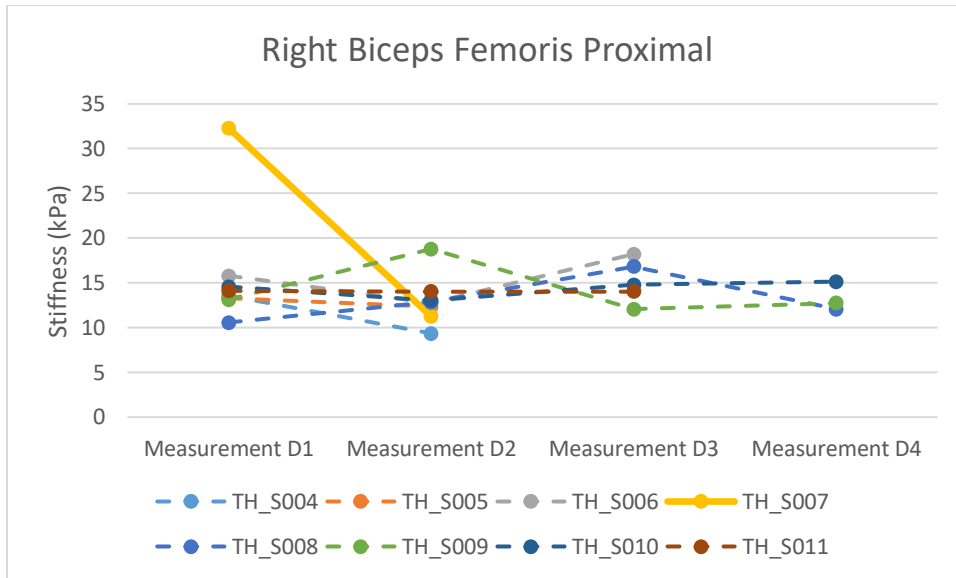


Figure 15: Individual Participant Right Biceps Femoris Proximal Stiffness Changes Throughout Competitive Season

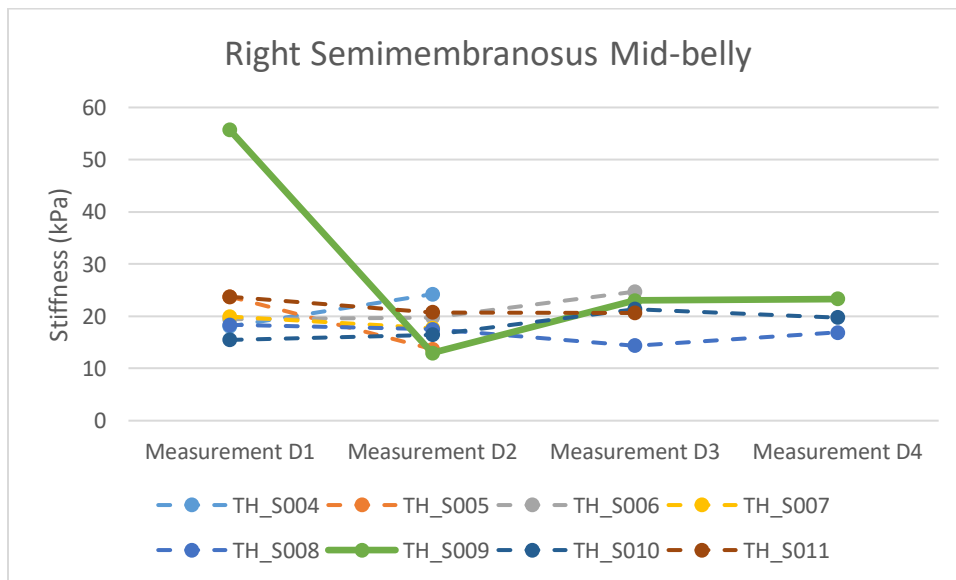


Figure 16: Individual Participant Right Semimembranosus Mid-Belly Stiffness Changes Throughout Competitive Season

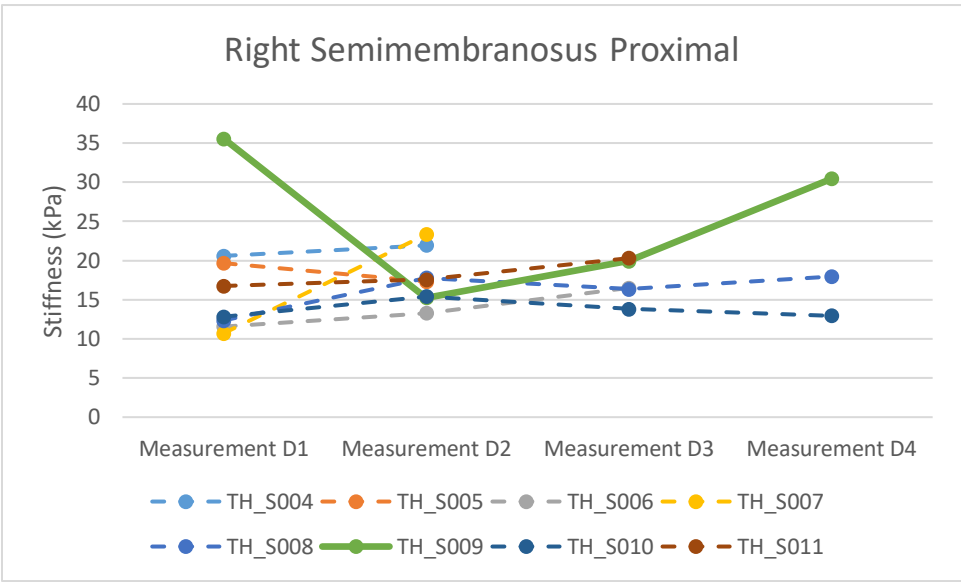


Figure 17: Individual Participant Right Semimembranosus Proximal Stiffness Changes Throughout Competitive Season

Tracking Mean Hamstring Stiffness Throughout Competitive Season

Analysis of mean hamstring stiffness data compared left and right leg stiffness for each hamstring muscle, by averaging each location (distal, mid-belly, and proximal) for each participant (N = 8). Table 6 shows mean stiffness results for biceps femoris muscles. Left biceps femoris muscle became stiffer across measurement days 1-4, mean stiffness peaked on day four, 16.09 ± 2.15 kPa (*figure 18*). Mean stiffness for right biceps femoris becomes less stiff across measurement days 1-4, with day one reporting highest stiffness values, 17.79 ± 4.68 kPa (*figure 18*). Table 7 shows mean stiffness results for semitendinosus muscles. Left semitendinosus muscle becomes slightly less stiff across measurement days, with highest stiffness values on day two, 21.35 ± 4.21 kPa (*figure 19*). Mean stiffness for right semitendinosus slightly decreased across measurement days; peak stiffness values occurring on day one, 20.54 ± 3.53 kPa (*figure 19*). Table 8 provides mean stiffness results for semimembranosus muscles. Left and right semimembranosus muscles each became less stiff across measurement days; peak stiffness values reached 19.19 ± 3.48 kPa and 20.57 ± 7.15 kPa occurring on day 1 for left and right semimembranosus muscles, respectively (*figure 20*). Examining figures 18-20, changes in stiffness across measurement days appear small. Comparing percent differences in mean stiffness changes from measurement day one to day four against our relative SEM value for muscle (4.55%) showed 5/6 (right semitendinosus was -1.46%) hamstring muscles had percent differences of 5% or greater. (*table 9*).

Table 6: Biceps Femoris Stiffness Across Measurement Days (kPa)

	Day 1		Day 2		Day 3		Day 4	
	Left	Right	Left	Right	Left	Right	Left	Right
S004	14.53	13.93	11.13	10.80				
S005	14.42	17.13	15.41	14.08				
S006	16.32	17.99	19.21	19.02	15.74	21.35		
S007	11.82	26.58	13.46	12.33				
S008	14.93	11.76	16.74	14.53	12.36	13.84	14.78	14.38
S009	19.58	14.51	17.44	18.77	20.22	13.80	18.57	17.33
S010	14.62	21.18	14.52	13.95	16.66	16.63	14.93	13.34
S011	15.78	19.21	18.11	14.72	15.08	14.32		
Mean	15.25	17.79	15.75	14.78	16.01	15.99	16.09	15.02
Std. Deviation	2.19	4.68	2.66	2.85	2.84	3.22	2.15	2.07

Table 7: Semitendinosus Stiffness Across Measurement Days (kPa)

	Day 1		Day 2		Day 3		Day 4	
	Left	Right	Left	Right	Left	Right	Left	Right
S004	13.34	15.86	14.24	14.26				
S005	24.60	22.02	23.35	18.41				
S006	19.19	20.06	21.29	20.61	19.48	18.12		
S007	21.42	20.11	20.63	20.18				
S008	23.42	20.75	25.77	22.22	21.30	18.25	21.18	23.78
S009	17.90	17.22	20.67	18.86	20.99	19.74	20.65	21.87
S010	16.69	20.59	17.59	17.96	13.73	13.16	16.51	15.08
S011	27.43	27.73	27.24	27.69	23.79	22.34		
Mean	20.50	20.54	21.35	20.02	19.86	18.32	19.45	20.24
Std. Deviation	4.60	3.53	4.21	3.88	3.76	3.35	2.56	4.57

Table 8: Semimembranosus Stiffness Across Measurement Days (kPa)

	Day 1		Day 2		Day 3		Day 4	
	Left	Right	Left	Right	Left	Right	Left	Right
S004	21.57	18.52	12.93	18.14				
S005	23.48	22.67	19.56	14.16				
S006	15.36	21.76	15.46	19.70	21.65	22.10		
S007	17.08	14.93	14.63	17.76				
S008	19.05	15.67	21.47	17.60	15.82	14.54	17.16	16.40
S009	24.05	36.21	17.82	13.92	18.35	19.58	18.63	22.48
S010	15.20	13.69	17.23	14.45	19.54	16.34	17.40	15.06
S011	17.74	21.12	21.19	18.03	18.47	19.68		
Mean	19.19	20.57	17.54	16.72	18.77	18.45	17.73	17.98
Std. Deviation	3.48	7.15	3.09	2.21	2.11	2.99	0.79	3.95

Table 9: Percent Differences Between Measurement Day 1 and Day 4 Means

Hamstring Muscle	Measurement Day 1 Mean Stiffness (kPa)	Measurement Day 4 Mean Stiffness (kPa)	Percent Differences
Left Biceps Femoris	15.25 (2.19)	16.09 (2.15)	5.50%
Right Biceps Femoris	17.79 (4.68)	15.02 (2.07)	-15.57%
Left Semitendinosus	20.50 (4.60)	19.45 (2.56)	-5.12%
Right Semitendinosus	20.54 (3.53)	20.24 (4.57)	-1.46%
Left Semimembranosus	19.19 (3.48)	17.73 (0.79)	-7.61%
Right Semimembranosus	20.57 (7.15)	17.98 (3.95)	-12.59%

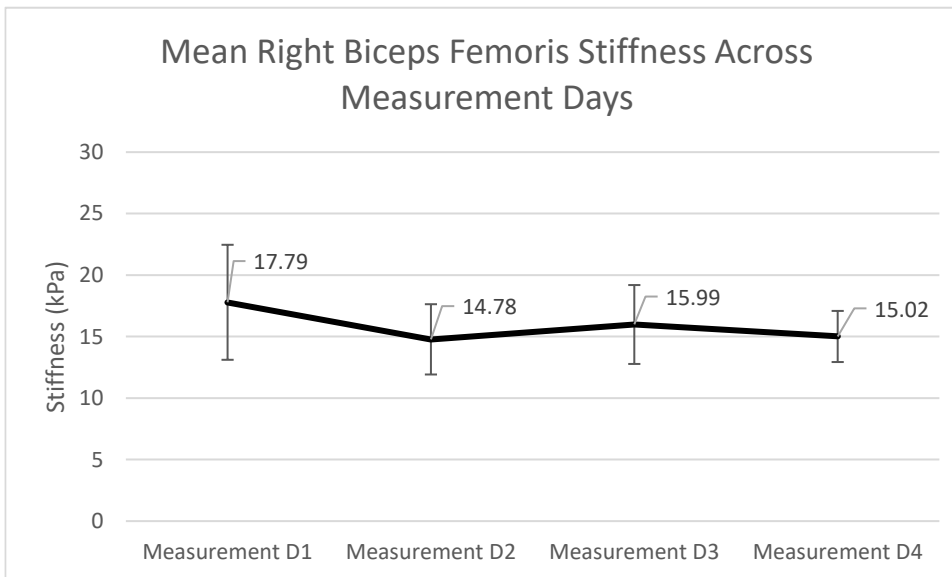
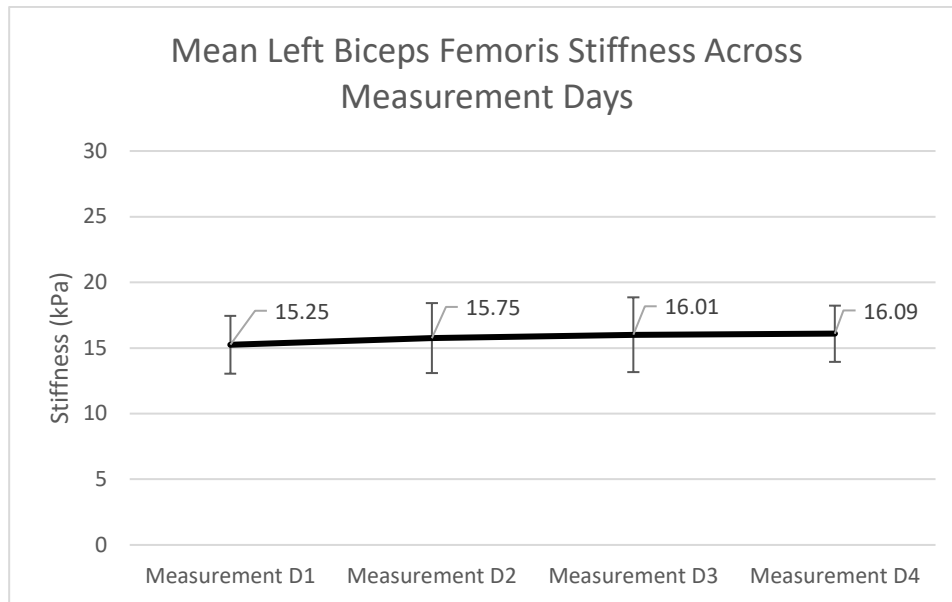


Figure 18: Mean Biceps Femoris Muscle Stiffness Throughout Competitive Season

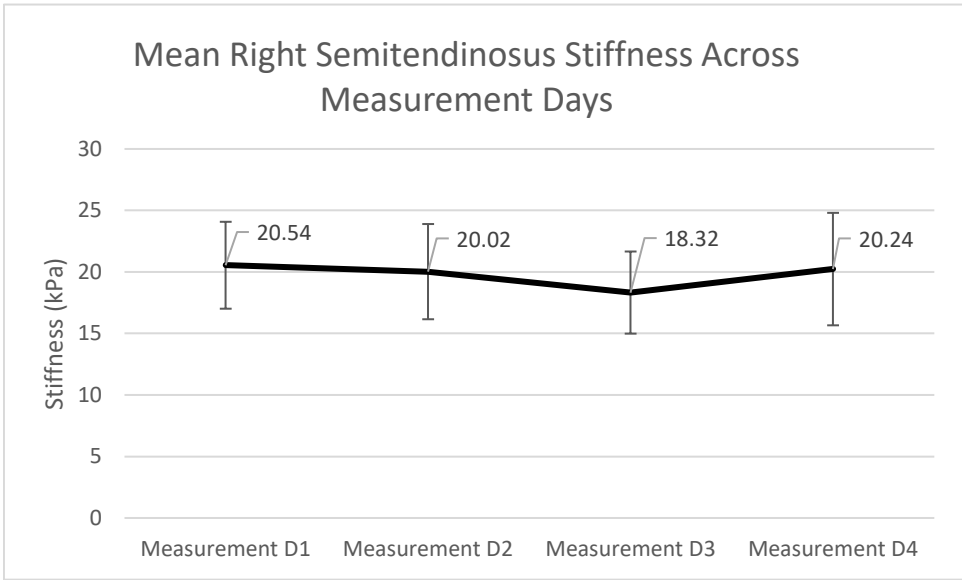
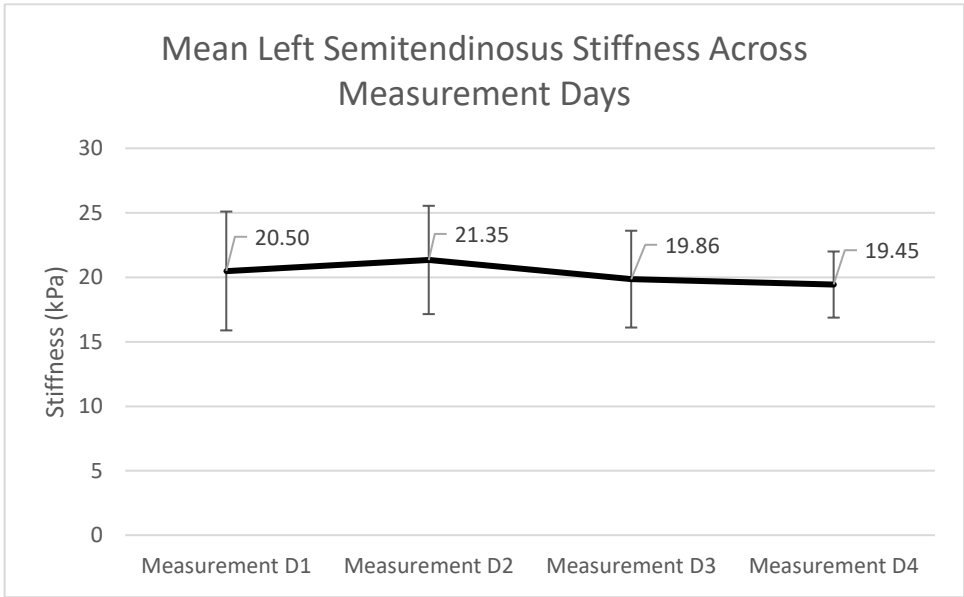


Figure 19: Mean Semitendinosus Muscle Stiffness Throughout Competitive Season

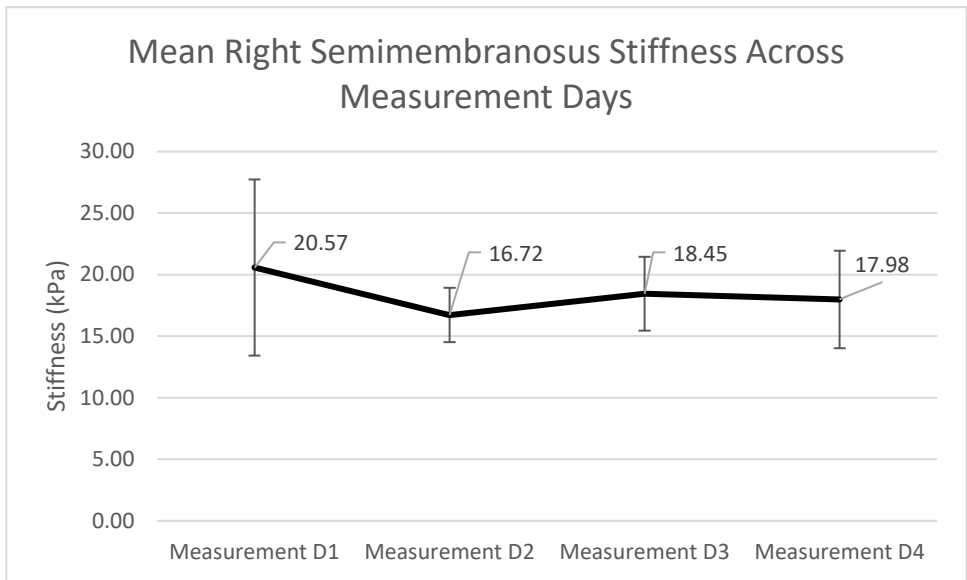
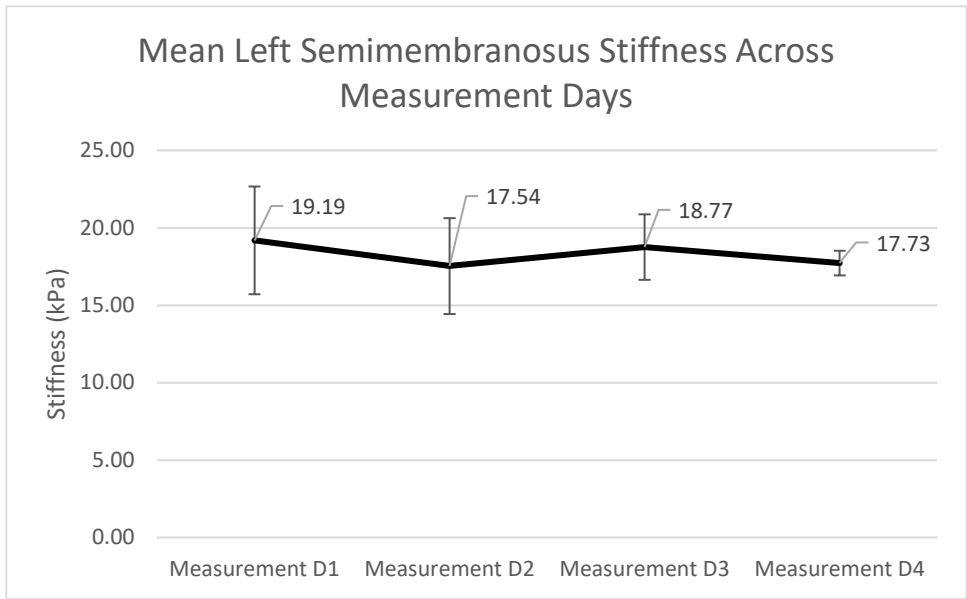


Figure 20: Mean Semimembranosus Muscle Stiffness Throughout Competitive Season

Chapter V. Discussion

Introduction

Ultrasound machines with SWE capability, specifically Supersonic Aixplorer, are expensive and force research laboratories and other clinical practices to operate utilizing one machine. As a result, researchers and clinicians conducting studies assessing multiple participants may end up monopolizing their ultrasound machine's usage; thus, not permitting simultaneous data processing and hindering research efficiency. Development of a custom algorithm that processes SWE data away from an ultrasound machine offers researchers and clinicians more time for data collections and can decrease time needed to process data.

The first part of this thesis developed a custom algorithm with the ability to consistently analyze SWE images and provided stiffness assessments for specified ROI's. Application of the newly validated custom algorithm to an existing data set was the second part of this thesis. Algorithm reliability results concluded excellent ICC and SEM values for muscle, tendon, and ligament. After establishing our code works and takes consistent measurements and validating it against the ultrasound machine, we applied the custom image processing algorithm and analyzed a pre-existing data set.

Established Reliability of Custom Algorithm

Inter-day reliability reported excellent values for all three tissue types; for muscle and tendon each reported ICC values of 0.999 and ligament reported a value of 0.998. We determined, a priori, SEM values above 5 kPa would be considered more than measurement error and an indication of programmatic errors within our custom algorithm. Each of our SEM for muscle (0.01 kPa), tendon (0.06 kPa), and ligament (0.14 kPa) were well below that threshold. The SEM values observed are postulated to be caused from differences in how the custom image

processing algorithm creates its ROI vs. how the ultrasound machine creates its ROI. Supersonic Aixplorer defines its ROI in the shape of a circle. In contrast, our custom algorithm defined its ROI in the shape of a rectangle. Based on the SEM values listed above, we believe these error values were caused by our custom algorithm using rectangles for ROI instead of circles. Each of the SEM calculations were below 1 kPa, thus reiterating the differing ROI shape did not substantially influence our custom algorithm's ability to produce comparable stiffness values to the ultrasound machine. Given the excellent SEM values reported in this thesis, it is plausible to presume if both measurement techniques had the same shaped ROI our algorithm would have produced more comparable stiffness values to the ultrasound machine.

Validated Custom Algorithm

Bland-Altman plots displayed no large offset from zero, indicated by small mean differences calculated in muscle (0.05 kPa), tendon (3.23 kPa), and ligament (5.32 kPa) (*figure 6-8*). Examining mean differences between both measurement techniques allowed us to confidently predict a 95% probability the stiffness difference between our custom algorithm and the ultrasound machine would be ± 0.77 kPa in muscle. For tendon, we confidently predicted a 95% probability the stiffness difference between our custom algorithm and the ultrasound machine would be ± 13.35 kPa. Ligament tissue data concluded we could confidently predict a 95% probability the stiffness difference between our custom algorithm and the ultrasound machine would be ± 20.01 kPa in ligament.

Comparing SWE imaging of muscle to tendon and ligament tissue displayed tendon and ligament had a much smaller range of similar tissue surrounding their structures. The lack of similar tissue surrounding these irregular structures possibly created a larger effect in stiffness assessment values. We postulate the larger mean difference values observed in tendon and

ligament are caused by an increased amount of dissimilar surrounding tissue being included in our ROI creation.

Hamstring Stiffness Gender Differences

Based on an effect size of 0.11, no small differences were observed when comparing male and female biceps femoris musculature. Both muscles, semitendinosus and semimembranosus, had small significant gender stiffness differences, effect sizes of 0.44 and 0.46, respectively. Figure 9 also showed semitendinosus muscle regardless of gender is the stiffer muscle in the hamstring muscle complex. Male athletes had stiffer semitendinosus muscles compared to female sprinter and jumpers. Male athletes having stiffer semitendinosus muscle is related to previous research that reported males have stiffer semitendinosus tendon than female counter parts (Itoigawa et al., 2018). Previous research literature also reported male athletes had higher injury rates for HSI's than female counterparts; findings in this thesis possibly provide insight as to why males have higher HSI incidence, due to having stiffer tissue (Edouard et al., 2016; D. A. Opar et al., 2014). Further research is needed on this topic to make that evidence conclusive.

HSI History vs. No Previous HSI History

Previous literature estimating stiffness from the frequency of oscillation of the shank about the ankle, found previously injured runners had greater plantar flexor musculotendinous stiffness than healthy athletes (Pamukoff & Blackburn, 2015). Our preliminary results yielded contrasting results; athletes with no previous history of HSI appeared to have a large significant difference in biceps femoris muscle (effect size 1.02) compared to athletes with a previous history of HSI's. Biceps femoris muscle being the most injured hamstring muscle may partially explain the effect size we calculated (Comin et al., 2013; Connell et al., 2004). No significant

differences were calculated in semitendinosus and semimembranosus muscle, effect sizes 0.20 and 0.06, respectively. There is some evidence that supports our findings that healthy tissue is stiffer than injury symptomatic tissue (Maquirriain, 2012). This study concluded athletes with Achilles tendinopathy had lower stiffness measurements possibly due to increasing ankle compliance (Maquirriain, 2012). We should note Maquirriain, 2012, measured stiffness in Achilles tendon by modeling vertical ground reaction force during hopping tasks. It is plausible athletes in our study with a history of HSI had lower stiffness values due to an increased compliance of the previously injured tissue, possibly a result from injury rehabilitation. Alternatively, because we do not know the hamstring stiffness before injury for the athletes with a history of HSI, we must consider the possibility these athletes may have had naturally less stiff tissue.

Individual Participant Outlier Analysis

One subject (S009) was diagnosed with a hamstring strain injury after day one data collection (Table 2). HSI was diagnosed by an athletic trainer as a grade I right hamstring strain injury. S009 was a 200- and 400-meter sprinter that had no previous history of HSI. SWE analysis of the right semimembranosus, at the mid-belly, revealed stiffness values unlike any other assessment from this dataset. Semimembranosus mid-belly stiffness assessments measured 55.69 kPa (*figure 13*). Compared to all other participants' semimembranosus mid-belly stiffness assessments, S009 stiffness measurements were 5.45 standard deviations above the mean (*figure 13*). It is worth noting that S009 proximal right semimembranosus also revealed a high stiffness measurement of 35.57 kPa (*figure 13*). When compared to all other participants' proximal semimembranosus assessments, S009 stiffness measurements were 3.64 standard deviations above the mean (*figure 13*).

Further analysis of hamstring stiffness data revealed eleven data points considered to be outliers when compared to mean values from each hamstring muscle at either location, including values from S009 injured semimembranosus mid-belly. Figure 11 shows biceps femoris muscle producing 6 outlier points, ranging from 2.1-4.86 standard deviations above mean values. Two of six biceps femoris outliers were from S007 right mid-belly and proximal muscle; measuring 33.76kPa (4.44 standard deviations above the mean) and 32.28kPa (4.86 standard deviations above the mean), respectively. Figure 13 shows semimembranosus muscle data producing 4 outliers, ranging 2.21-3.64 standard deviations away from mean values, not including injury data from S009.

Even though the stiffness measurements from the ten outliers did not cause injury, based on preliminary analysis it is plausible these outliers may indicate early onset microscopic damage within muscle fibers. We postulate SWE assessment of muscle stiffness revealing values 3 standard deviations beyond normal stiffness values, may be a possible accumulation of strain threshold indicator that may assist in identifying potential injury risks. Based on the interpretation of the preliminary data, we can potentially say athletes exhibiting stiffness values more than 3 standard deviations above the mean, represent an accumulation of microscopic damage within muscle tissue, but not substantial enough to cause major injury. We also postulate athletes exhibiting stiffness values more than 5 standard deviations from the mean, may be at an increased risk for potential muscular strain injury and intervention should be considered to avoid injury.

Tracking Hamstring Stiffness Throughout Competitive Season

Plotting individual participant stiffness data across measurement days for each muscle at all three locations (distal, mid-belly, proximal), allowed any alterations occurring within muscle

to be observed more easily. Generally, figure 14 demonstrates how participants' hamstring stiffness changed throughout the competitive season; stiffness ranges between 12-23kPa. Fluctuations in hamstring stiffness were evident but did not produce injury (*figure 14*). These changes appeared to be normal and a result of normal musculature responses to an athletes' varying in-season training and/or competition schedule. Remaining individual hamstring stiffness plots that did not produce an injury or display stiffness values more than three standard deviations above mean can be found within appendix A. Conversely, figures 15-17 reveal changes in hamstring stiffness values throughout the competitive season; these changes are another representation of the outlier data previously mentioned. Based on S009 injury data point we believe the outliers give us some insight into muscle material properties prior to injury and individual line plots of hamstring stiffness data at specific locations, allow us to examine how muscles respond before and after elevated stiffness levels.

Seasonal Effect on Mean Hamstring Stiffness

Based on 5/6 hamstring muscles we analyzed having percent differences of 5% or greater, we believe the changes observed in mean hamstring stiffness across measurement days are real because they exceed the calculated 4.55% relative SEM for muscle tissue. After examining stiffness values from each individual hamstring muscle across all measurement days, it appears left and right semitendinosus muscle was stiffer than biceps femoris and semimembranosus muscles. Despite being stiffer, semitendinosus muscle data did not reveal any accumulation of damage or injury outliers from our outlier analysis. This may be explained by previous literature reporting semitendinosus muscle is the least injured hamstring muscle, biceps femoris 84%, semimembranosus 11%, and semitendinosus 4% (Comin et al., 2013; Connell et al., 2004; Ekstrand, Lee, et al., 2016). It is possible the stiffer muscle observed in the

semitendinosus may act to protect that muscle from injury, potentially reducing injury incidence within the muscle. We speculate muscular strain injuries could be altering the structural integrity of tissue. These alterations could be developing weak points, post-injury, causing muscle tissue to be less stiff and thus leaving that tissue at an increased risk of injury.

Areas for Future Research

This thesis successfully created a custom SWE image processing algorithm; capable of assessing stiffness values in muscle, tendon, and ligament tissues. Future SWE studies measuring stiffness in any other additional soft tissue structures, can use this new algorithm to process elastography imaging data.

Participant S009 displayed substantial differences in stiffness of their injured semimembranosus mid-belly compared to other participants' data. It is plausible that measuring stiffness of injured muscles immediately following muscular strain could show stiffness values higher than 5 standard deviations above the mean. The ability to track microscopic damage may assist in injury recovery process; tracking stiffness in rehabilitated muscles can help athletic training personnel quantitatively determine when an athlete can safely return to activity. Future studies monitoring stiffness of injured athletes should implement daily SWE assessment to better understand how stiffness of injured tissue recovers.

Identifying at risk athletes, through careful monitoring of muscle stiffness, can possibly help athletic training personnel prevent major muscular injury in athletes (Sadeghi, Lin, et al., 2018). This thesis identified potential accumulation of muscular strain threshold (three or more SD above the mean) and potential muscular injury threshold (5 or more SD above the mean). Future research focused on SWE stiffness assessment immediately following an injury may provide baseline stiffness values that can be useful in interpreting potential stiffness outliers,

like the outliers identified in this thesis. A prospective study utilizing SWE to monitor athletes that have suffered a muscular injury can provide insight into if the thresholds identified by our outlier analysis are true; if these injury thresholds are true then these values can be used in identifying at risk athletes in future research. .

Limitations

There were some limitations to this thesis, first being a small sample size. Of the original 14 participants in this pre-existing dataset, only eight were included in the analysis of tracking stiffness throughout the competitive season. Subjects from this dataset were recruited from a single track & field team; allowing us to include sprinter and jumping athletes of similar age and skill level that met our inclusion criteria.

Secondly, there is a risk of hamstring stiffness becoming altered in some capacity by in-season resistance training. Daily variations in training formats and intensities may influence hamstring muscle stiffness. Information detailing daily training regimens was not disclosed in this dataset. Knowing specific daily activities of athletes may provide more insight into muscle stiffness changes within individual athletes across measurement days.

Lastly, the ultrasound machine defines its ROI in circles, while our custom algorithm defines ROI in the shape of rectangles. Our custom algorithm still demonstrated it can produce similar stiffness values compared to the ultrasound machine's stiffness values in multiple tissue types, despite this distinction (*figure 6-8*). We believe the mean percent error values from our validation analysis is a result of this ROI difference. If the ultrasound machine and our custom algorithm defined ROI using the same shape, we believe the mean percent error values would be less than the values reported earlier, suggesting an even better match of stiffness values between both measurement techniques.

Conclusion

We developed a working algorithm that analyzed stiffness in SWE images and successfully validated our code against three tissue types. Our custom SWE image processing program algorithm will allow researchers and clinicians to process images away from the ultrasound machine; thus, increasing opportunities for data collections and make data processing faster. Application of the custom SWE processing algorithm allowed us to analyze a dataset unable to be completely processed on the ultrasound machine.

Examining individual participants' hamstring stiffness throughout the competitive season yielded preliminary results showing significant changes in muscle stiffness. Hamstring muscle stiffness values more than three standard deviations above the mean may be an indication of accumulation of strain; however, it appears not substantial enough to increase eminent muscular injury risk. Hamstring stiffness value more than five standard deviations above the mean may have been the cause of muscle injury seen in S009. We believe the preliminary results from this thesis justify regular monitoring of athlete's hamstring muscle stiffness, because it appears there is highly increased stiffness prior to injury. A prospective study aimed at close monitoring of athletes' hamstring stiffness changes can help identify those individuals at risk of injuring their hamstrings.

References

- Alonso, J. M., Edouard, P., Fischetto, G., Adams, B., Depiesse, F., & Mountjoy, M. (2012). Determination of future prevention strategies in elite track and field: Analysis of Daegu 2011 IAAF Championships injuries and illnesses surveillance. *British Journal of Sports Medicine*, *46*(7), 505–514. <https://doi.org/10.1136/bjsports-2012-091008>
- Alonso, J. M., Junge, A., Renström, P., Engebretsen, L., Mountjoy, M., & Dvorak, J. (2009). Sports injuries surveillance during the 2007 IAAF world athletics championships. *Clinical Journal of Sport Medicine*, *19*(1), 26–32. <https://doi.org/10.1097/JSM.0b013e318191c8e7>
- Alonso, J. M., Tscholl, P. M., Engebretsen, L., Mountjoy, M., Dvorak, J., & Junge, A. (2010). Occurrence of injuries and illnesses during the 2009 IAAF World Athletics Championships. *British Journal of Sports Medicine*, *44*(15), 1100–1105. <https://doi.org/10.1136/bjism.2010.078030>
- Andonian, P., Viallon, M., Le Goff, C., De Bourguignon, C., Tourel, C., Morel, J., Giardini, G., Gergeli, L., Millet, G. P., & Croisille, P. (2016). Correction: Shear-wave elastography assessments of quadriceps stiffness changes prior to, during and after prolonged exercise: A longitudinal study during an extreme mountain ultra-marathon (PLoS ONE (2016) 11:8 (e0161855) DOI: 10.1371/journal.pone.016185. *PLoS ONE*, *11*(11), 1–21. <https://doi.org/10.1371/journal.pone.0167668>
- Arnason, A., Andersen, T. E., Holme, I., Engebretsen, L., & Bahr, R. (2008). Prevention of hamstring strains in elite soccer: An intervention study. *Scandinavian Journal of Medicine and Science in Sports*, *18*(1), 40–48. <https://doi.org/10.1111/j.1600-0838.2006.00634.x>
- Askling, C. M., Tengvar, M., Saartok, T., & Thorstensson, A. (2007a). Acute first-time hamstring strains during high-speed running: A longitudinal study including clinical and magnetic resonance imaging findings. *American Journal of Sports Medicine*. <https://doi.org/10.1177/0363546506294679>
- Askling, C. M., Tengvar, M., Saartok, T., & Thorstensson, A. (2007b). Acute first-time hamstring strains during slow-speed stretching: Clinical, magnetic resonance imaging, and recovery characteristics. *American Journal of Sports Medicine*. <https://doi.org/10.1177/0363546507303563>
- Basford, J. R., Jenkyn, T. R., An, K. N., Ehman, R. L., Heers, G., & Kaufman, K. R. (2002). Evaluation of healthy and diseased muscle with magnetic resonance elastography. *Archives of Physical Medicine and Rehabilitation*, *83*(11), 1530–1536. <https://doi.org/10.1053/apmr.2002.35472>
- Bercoff, J., Tanter, M., & Fink, M. (2004). Supersonic Shear Imaging: A New Technique for Soft Tissue Elasticity Mapping. *IEEE Transactions on Ultrasonics, Ferroelectrics, and Frequency Control*, *51*(4), 396–409. <https://doi.org/10.1109/TUFFC.2004.1295425>
- Blackburn, J. T., Bell, D. R., Norcross, M. F., Hudson, J. D., & Kimsey, M. H. (2009). Sex comparison of hamstring structural and material properties. *Clinical Biomechanics*, *24*(1), 65–70. <https://doi.org/10.1016/j.clinbiomech.2008.10.001>
- Brockett, C. L., Morgan, D. L., & Proske, U. (2001). Human hamstring muscles adapt to eccentric exercise by changing optimum length. *Medicine and Science in Sports and Exercise*, *33*(5), 783–790. <https://doi.org/10.1097/00005768-200105000-00017>
- Brockett, C. L., Morgan, D. L., & Proske, U. (2004). Predicting Hamstring Injury in Elite Athletes. *Medicine and Science in Sports and Exercise*, *36*(3), 379–387. <https://doi.org/10.1249/01.MSS.0000117165.75832.05>

- Brockett, Camilla L., Morgan, D. L., & Proske, U. (2004). Predicting Hamstring Injury in Elite Athletes. *Medicine and Science in Sports and Exercise*, 36(3), 379–387. <https://doi.org/10.1249/01.MSS.0000117165.75832.05>
- Brooks, S. V., Zerba, E., & Faulkner, J. A. (1995). Injury to muscle fibres after single stretches of passive and maximally stimulated muscles in mice. *The Journal of Physiology*, 488(2), 459–469. <https://doi.org/10.1113/jphysiol.1995.sp020980>
- Brooks, Susan V., & Faulkner, J. A. (1996). The magnitude of the initial injury induced by stretches of maximally activated muscle fibres of mice and rats increases in old age. *Journal of Physiology*, 497(2), 573–580. <https://doi.org/10.1113/jphysiol.1996.sp021790>
- Camp, C. L., Dines, J. S., van der List, J. P., Conte, S., Conway, J., Altchek, D. W., Coleman, S. H., & Pearle, A. D. (2018). Summative Report on Time Out of Play for Major and Minor League Baseball: An Analysis of 49,955 Injuries From 2011 Through 2016. *The American Journal of Sports Medicine*, 036354651876515. <https://doi.org/10.1177/0363546518765158>
- Clark, R. A. (2008). Hamstring injuries: Risk assessment and injury prevention. In *Annals Academy of Medicine Singapore* (pp. 341–346). <https://doi.org/10.3109/09593985.2016.1138347>
- Comin, J., Malliaras, P., Baquie, P., Barbour, T., & Connell, D. (2013). *Return to Competitive Play After Hamstring Injuries Involving Disruption of the Central Tendon*. 41(1). <https://doi.org/10.1177/0363546512463679>
- Connell, D. A., Schneider-Kolsky, M. E., Hoving, J. L., Malara, F., Buchbinder, R., Koulouris, G., Burke, F., & Bass, C. (2004). Longitudinal study comparing sonographic and MRI assessments of acute and healing hamstring injuries. *American Journal of Roentgenology*, 183(4), 975–984. <https://doi.org/10.2214/ajr.183.4.1830975>
- Crema, M. D., Jarraya, M., Engebretsen, L., Roemer, F. W., Hayashi, D., Domingues, R., Skaf, A. Y., & Guermazi, A. (2018). Imaging-detected acute muscle injuries in athletes participating in the Rio de Janeiro 2016 Summer Olympic Games. *British Journal of Sports Medicine*, 52(7), 460–464. <https://doi.org/10.1136/bjsports-2017-098247>
- Dalton, S. L., Kerr, Z. Y., & Dompier, T. P. (2015). Epidemiology of hamstring strains in 25 NCAA sports in the 2009-2010 to 2013-2014 academic years. *American Journal of Sports Medicine*, 43(11), 2671–2679. <https://doi.org/10.1177/0363546515599631>
- De Smet, A. A., & Best, T. M. (2000). MR imaging of the distribution and location of acute hamstring injuries in athletes. *American Journal of Roentgenology*, 174(2), 393–399. <https://doi.org/10.2214/ajr.174.2.1740393>
- Dresner, A. M., Rose, G. H., Rossman, P. J., Murhupillai, R., Manduca, A., & Ehman, R. L. (2001). Magnetic resonance elastography of skeletal muscle. *Journal of Magnetic Resonance Imaging*, 13, 269–276.
- Dubois, G., Kheireddine, W., Vergari, C., Bonneau, D., Thoreux, P., Rouch, P., Tanter, M., Gennisson, J. L., & Skalli, W. (2015). Reliable Protocol for Shear Wave Elastography of Lower Limb Muscles at Rest and During Passive Stretching. *Ultrasound in Medicine and Biology*, 41(9), 2284–2291. <https://doi.org/10.1016/j.ultrasmedbio.2015.04.020>
- Edouard, P., Branco, P., & Alonso, J. M. (2016). Muscle injury is the principal injury type and hamstring muscle injury is the first injury diagnosis during top-level international athletics championships between 2007 and 2015. *British Journal of Sports Medicine*, 50(10), 619–630. <https://doi.org/10.1136/bjsports-2015-095559>
- Edouard, P., Depiesse, F., Branco, P., & Alonso, J. M. (2014). Analyses of Helsinki 2012 European athletics championships injury and illness surveillance to discuss elite athletes

- risk factors. *Clinical Journal of Sport Medicine*, 24(5), 409–415.
<https://doi.org/10.1097/JSM.0000000000000052>
- Ekstrand, J., Hägglund, M., & Waldén, M. (2011). Epidemiology of muscle injuries in professional football (soccer). *American Journal of Sports Medicine*, 39(6), 1226–1232.
<https://doi.org/10.1177/0363546510395879>
- Ekstrand, J., Lee, J. C., & Healy, J. C. (2016). *MRI findings and return to play in football : a prospective analysis of 255 hamstring injuries in the UEFA Elite Club Injury Study*. 738–743. <https://doi.org/10.1136/bjsports-2016-095974>
- Ekstrand, J., Waldén, M., & Hägglund, M. (2016). Hamstring injuries have increased by 4% annually in men’s professional football, since 2001: A 13-year longitudinal analysis of the UEFA Elite Club injury study. *British Journal of Sports Medicine*, 50(12), 731–737.
<https://doi.org/10.1136/bjsports-2015-095359>
- Elliott, M. C. C. W., Zarins, B., Powell, J. W., & Kenyon, C. D. (2011). Hamstring muscle strains in professional football players: A 10-year review. *American Journal of Sports Medicine*, 39(4), 843–850. <https://doi.org/10.1177/0363546510394647>
- Feeley, B. T., Kennelly, S., Barnes, R. P., Muller, M. S., Kelly, B. T., Rodeo, S. A., & Warren, R. F. (2008). Epidemiology of National Football League Training Camp Injuries From 1998 to 2007. *The American Journal of Sports Medicine*, 36(8), 1597–1603.
<https://doi.org/10.1177/0363546508316021>
- Fitzharris, N., Jones, G., Jones, A., & Francis, P. (2017). The first prospective injury audit of League of Ireland footballers. *BMJ Open Sport & Exercise Medicine*, 3(1), e000220.
<https://doi.org/10.1136/bmjsem-2017-000220>
- Friden, J., Sjöstrom, M., & Ekblom, B. (1983). Myofibrillar damage following intense eccentric exercise in man. *International Journal of Sports Medicine*, 4(3), 170–176.
<https://doi.org/10.1055/s-2008-1026030>
- Gabbe, B. J., Finch, C. F., Bennell, K. L., & Wajswelner, H. (2005). Risk factors for hamstring injuries in community level Australian football. *British Journal of Sports Medicine*, 39(2), 106–110. <https://doi.org/10.1136/bjsem.2003.011197>
- Garrett, W. E. (1990). *Muscle strain injuries: clinical and basic aspects*.
- Gatos, I., Tsantis, S., Spiliopoulos, S., Karnabatidis, D., Theotokas, I., Zoumpoulis, P., Loupas, T., Hazle, J. D., & Kagadis, G. C. (2016). A new computer aided diagnosis system for evaluation of chronic liver disease with ultrasound shear wave elastography imaging. *Medical Physics*, 43(3), 1428–1436. <https://doi.org/10.1118/1.4942383>
- Gatos, I., Tsantis, S., Spiliopoulos, S., Karnabatidis, D., Theotokas, I., Zoumpoulis, P., Loupas, T., Hazle, J. D., & Kagadis, G. C. (2017). A Machine-Learning Algorithm Toward Color Analysis for Chronic Liver Disease Classification, Employing Ultrasound Shear Wave Elastography. *Ultrasound in Medicine and Biology*, 43(9), 1797–1810.
<https://doi.org/10.1016/j.ultrasmedbio.2017.05.002>
- Greenleaf, J. F., Fatemi, M., & Insana, M. (2003). Selected Methods for Imaging Elastic Properties of Biological Tissues. *Annual Review of Biomedical Engineering*, 5(1), 57–78.
<https://doi.org/10.1146/annurev.bioeng.5.040202.121623>
- Heiderscheid, B. C., Hoerth, D. M., Chumanov, E. S., Swanson, S. C., Thelen, B. J., & Thelen, D. G. (2005). Identifying the time of occurrence of a hamstring strain injury during treadmill running: A case study. *Clinical Biomechanics*.
<https://doi.org/10.1016/j.clinbiomech.2005.07.005>
- Hickey, J., Shield, A. J., Williams, M. D., & Opar, D. A. (2014). The financial cost of hamstring

- strain injuries in the Australian Football League. *British Journal of Sports Medicine*, 48(8), 729–730. <https://doi.org/10.1136/bjsports-2013-092884>
- Hincapié, C. A., Morton, E. J., & Cassidy, J. D. (2008). Musculoskeletal Injuries and Pain in Dancers: A Systematic Review. *Archives of Physical Medicine and Rehabilitation*, 89(9). <https://doi.org/10.1016/j.apmr.2008.02.020>
- Hootman, J. M., Dick, R., & Agel, J. (2007). Epidemiology of collegiate injuries for 15 sports: Summary and recommendations for injury prevention initiatives. *Journal of Athletic Training*, 42(2), 311–319. <https://doi.org/10.1111/j.1600-0838.2006.00528.x>
- Itoigawa, Y., Takazawa, Y., Maruyama, Y., Yoshida, K., Sakai, T., Ichimura, K., & Kaneko, K. (2018). A new technique of surgical planning for anterior cruciate ligament reconstruction: Feasibility Assessment of Shear Wave Elastography to Tendon of Semitendinosus Muscle. *Clinical Anatomy*. <https://doi.org/10.1002/ca.23000>
- Jones, C., Allen, T., Talbot, J., Morgan, D. L., & Proske, U. (1997). Changes in the mechanical properties of human and amphibian muscle after eccentric exercise. *European Journal of Applied Physiology and Occupational Physiology*, 76(1), 21–31.
- Kim, K., Hwang, H. J., Kim, S. G., Lee, J. H., & Jeong, W. K. (2018). Can shoulder muscle activity be evaluated with ultrasound shear wave elastography? *Clinical Orthopaedics and Related Research*, 476(6), 1276–1283. <https://doi.org/10.1097/01.blo.0000533628.06091.0a>
- Koulouris, G., & Connell, D. (2003). Evaluation of the hamstring muscle complex following acute injury. *Skeletal Radiology*, 32(10), 582–589. <https://doi.org/10.1007/s00256-003-0674-5>
- Koulouris, G., Connell, D. A., Brukner, P., & Schneider-Kolsky, M. (2007). Magnetic resonance imaging parameters for assessing risk of recurrent hamstring injuries in elite athletes. *American Journal of Sports Medicine*, 35(9), 1500–1506. <https://doi.org/10.1177/0363546507301258>
- Lacourpaille, L., Hug, F., Bouillard, K., Hogrel, J. Y., & Nordez, A. (2012). Supersonic shear imaging provides a reliable measurement of resting muscle shear elastic modulus. *Physiological Measurement*, 33(3), N19–N28. <https://doi.org/10.1088/0967-3334/33/3/N19>
- Lieber, R. L., & Fridén, J. (1993). Muscle damage is not a function of muscle force but active muscle strain. *Journal of Applied Physiology*, 74(2), 520–526.
- Lynn, R., & Morgan, D. L. (1994). Decline running produces more sarcomeres in rat vastus intermedius muscle fibers than does incline running. *Journal of Applied Physiology*, 77(3), 1439–1444. <https://doi.org/10.1152/jappl.1994.77.3.1439>
- Lynn, R., Talbot, J. A., & Morgan, D. L. (1998). Differences in rat skeletal muscles after incline and decline running. *Journal of Applied Physiology*, 85(1), 98–104. <https://doi.org/10.1152/jappl.1998.85.1.98>
- Malliaropoulos, N., Papacostas, E., Kiritsi, O., Papalada, A., Gougoulas, N., & Maffulli, N. (2010). Posterior thigh muscle injuries in elite track and field athletes. *American Journal of Sports Medicine*, 38(9), 1813–1819. <https://doi.org/10.1177/0363546510366423>
- Maquirriain, J. (2012). Leg stiffness changes in athletes with achilles tendinopathy. *International Journal of Sports Medicine*. <https://doi.org/10.1055/s-0032-1304644>
- Mendes, B., Firmino, T., Oliveira, R., Neto, T., Infante, J., Vaz, J. R., & Freitas, S. R. (2018). Hamstring stiffness pattern during contraction in healthy individuals: analysis by ultrasound-based shear wave elastography. *European Journal of Applied Physiology*, 118(11), 2403–2415. <https://doi.org/10.1007/s00421-018-3967-z>
- Morgan, D. L. (1990). New insights into the behavior of muscle during active lengthening.

- Biophysical Journal*, 57(2), 209–221. [https://doi.org/10.1016/S0006-3495\(90\)82524-8](https://doi.org/10.1016/S0006-3495(90)82524-8)
- Muthupillai, R., Lomas, D. J., Rossman, P. J., Greenleaf, J. F., Manduca, A., & Ehman, R. L. (1995). Magnetic Resonance Elastography by Direct Visualization of Propagating Acoustic Strain Waves. *Science*, 269(September), 1854–1857. <https://doi.org/10.1126/science.7569924>
- Noonan, T. J., Best, T. M., Seaber, A. V., & Garrett, W. E. (1994). Identification of muscle injury a threshold for skeletal muscle injury. *American Journal of Sports Medicine*, 22(2), 257–261. <https://doi.org/10.1177/036354659402200217>
- Nordez, A., & Hug, F. (2010). Muscle shear elastic modulus measured using supersonic shear imaging is highly related to muscle activity level. *Journal of Applied Physiology*, 108(5), 1389–1394. <https://doi.org/10.1152/jappphysiol.01323.2009>
- Opar, D. A., Drezner, J., Shield, A., Williams, M., Webner, D., Sennett, B., Kapur, R., Cohen, M., Ulager, J., Cafengiu, A., & Cronholm, P. F. (2014). Acute hamstring strain injury in track-and-field athletes: A 3-year observational study at the Penn Relay Carnival. *Scandinavian Journal of Medicine and Science in Sports*, 24(4), 254–259. <https://doi.org/10.1111/sms.12159>
- Opar, David A., Williams, M. D., & Shield, A. J. (2012). Hamstring strain injuries: Factors that Lead to injury and re-Injury. *Sports Medicine*, 42(3), 209–226. <https://doi.org/10.2165/11594800-000000000-00000>
- Ophir, J., Cespedes, I., Ponnekanti, H., Yazdi, Y., & Li, X. (1991). Elastography: a Quantitative Method for Imaging the Elasticity of Biological Tissues. *Ultrasonic Imaging*, 13, 111–134.
- Ophir, Jonathan, Alam, S. K., Garra, B. S., Kallel, F., Konofagou, E. E., Krouskop, T., Merritt, C. R. B., Righetti, R., Souchon, R., Srinivasan, S., & Varghese, T. (2002). Elastography: Imaging the elastic properties of soft tissues with ultrasound. *Journal of Medical Ultrasonics*, 29(4), 155–171. <https://doi.org/10.1007/BF02480847>
- Orchard, J., & Best, M. T. (2002). The Management of Muscle Strain Injuries: An Early Return Versus the Risk of Recurrence. *Clinical Journal of Sport Medicine*, 12(1), 3–5. <https://oce.ovid.com/article/00042752-200201000-00004/HTML>
- Orchard, J., & Seward, H. (2002). Epidemiology of injuries in the Australian Football League, seasons 1997 – 2000. *Sports Medicine*, 39–45.
- Orchard, J. W., Seward, H., & Orchard, J. J. (2013). Results of 2 decades of injury surveillance and public release of data in the Australian Football League. *American Journal of Sports Medicine*, 41(4), 734–741. <https://doi.org/10.1177/0363546513476270>
- Pamukoff, D. N., & Blackburn, J. T. (2015). *Comparison of Plantar Flexor Musculotendinous Stiffness , Geometry , and Comparison of Plantar Flexor Musculotendinous Stiffness , Geometry , and Architecture in Male Runners With and Without a History of Tibial Stress Fracture*. April. <https://doi.org/10.1123/jab.2014-0127>
- Petersen, J., Thorborg, K., Nielsen, M. B., Budtz-Jørgensen, E., & Hölmich, P. (2011). Preventive effect of eccentric training on acute hamstring injuries in Men’s soccer: A cluster-randomized controlled trial. *American Journal of Sports Medicine*, 39(11), 2296–2303. <https://doi.org/10.1177/0363546511419277>
- Proske, U., & Morgan, D. L. (2001). Muscle damage from eccentric exercise: Mechanism, mechanical signs, adaptations and clinical applications. *Journal of Physiology*, 537(2), 333–345. <https://doi.org/10.1111/j.1469-7793.2001.00333.x>
- Rosenthal, J. A. (1996). Qualitative Descriptors of Strength of Association and Effect Size Qualitative Descriptors of Strength of Association and Effect Size. 8376.

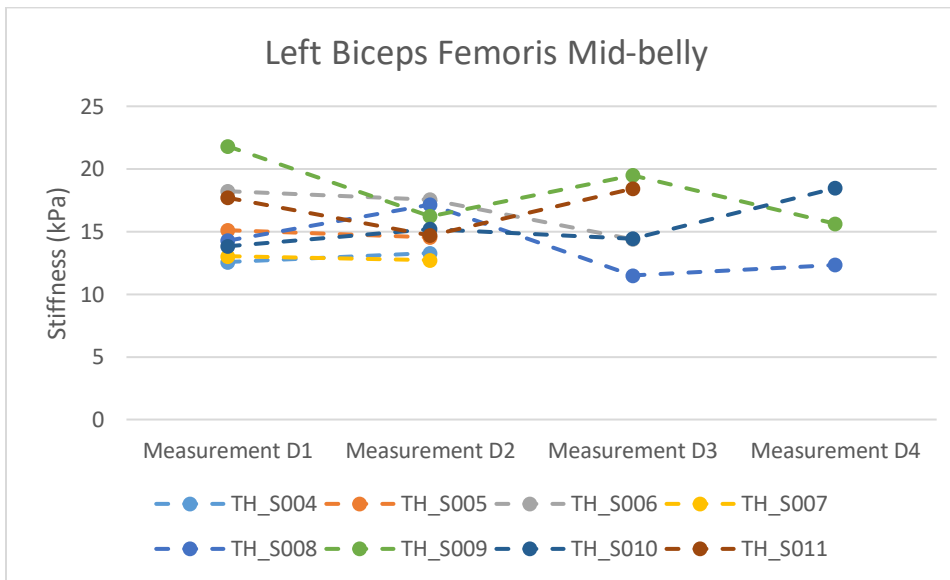
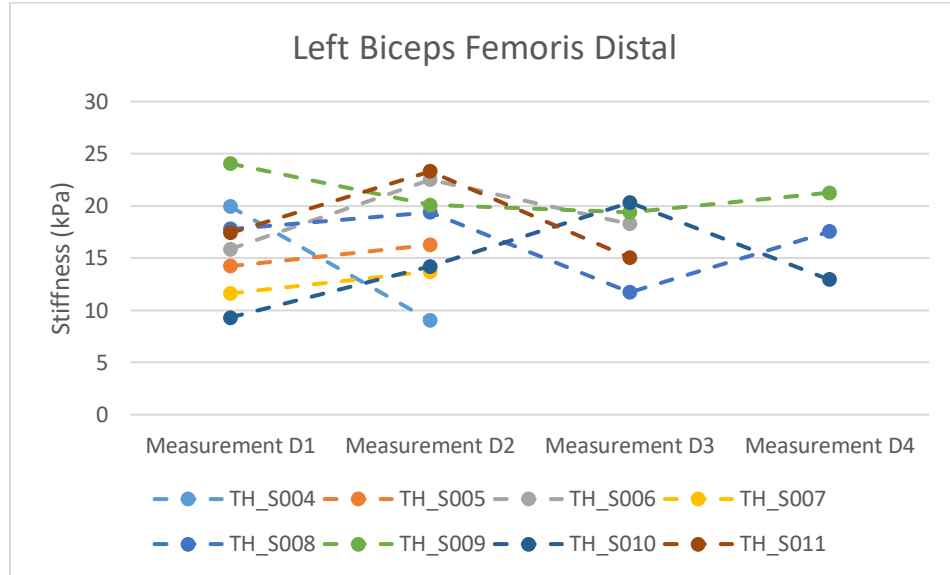
- <https://doi.org/10.1300/J079v21n04>
- Sadeghi, S., Lin, C., Bader, D. A., & Cortes, D. H. (2018). Evaluating Changes in Shear Modulus of Elbow Ulnar Collateral Ligament in Overhead Throwing Athletes Over the Course of a Competitive Season. *Journal of Engineering and Science in Medical Diagnostics and Therapy*, 1(4). <https://doi.org/10.1115/1.4041503>
- Sadeghi, S., Newman, C., & Cortes, D. H. (2018). Change in skeletal muscle stiffness after running competition is dependent on both running distance and recovery time: a pilot study. *PeerJ*, 6, 4469. <https://doi.org/10.7717/peerj.4469>
- Sarvazyan, A. P., Rudenko, O. V. ., Swanson, S. D., & Fowlkes, J. B. F. (1998). Shear Wave Elasticity Imaging: A New Ultrasonic Technology Of Medical Diagnostics. 24(9), 1419–1435. <https://doi.org/10.1175/MWR-D-17-0061.1>
- Schache, A. G., Dorn, T. W., Blanch, P. D., Brown, N. A. T., & Pandy, M. G. (2012). Mechanics of the human hamstring muscles during sprinting. *Medicine and Science in Sports and Exercise*, 44(4), 647–658. <https://doi.org/10.1249/MSS.0b013e318236a3d2>
- Schache, A. G., Kim, H. J., Morgan, D. L., & Pandy, M. G. (2010). Hamstring muscle forces prior to and immediately following an acute sprinting-related muscle strain injury. *Gait and Posture*, 32(1), 136–140. <https://doi.org/10.1016/j.gaitpost.2010.03.006>
- Schache, A. G., Wrigley, T. V., Baker, R., & Pandy, M. G. (2009). Biomechanical response to hamstring muscle strain injury. *Gait and Posture*. <https://doi.org/10.1016/j.gaitpost.2008.10.054>
- Seymore, K. D., Domire, Z. J., DeVita, P., Rider, P. M., & Kulas, A. S. (2017). The effect of Nordic hamstring strength training on muscle architecture, stiffness, and strength. *European Journal of Applied Physiology*, 117(5), 943–953. <https://doi.org/10.1007/s00421-017-3583-3>
- Shinohara, M., Sabra, K., Gennisson, J. L., Fink, M., & Tanter, M. L. (2010). Real-time visualization of muscle stiffness distribution with ultrasound shear wave imaging during muscle contraction. *Muscle and Nerve*, 42(3), 438–441. <https://doi.org/10.1002/mus.21723>
- Suga, M., Matsuda, T., Minato, K., Oshiro, O., Chihara, K., Okamoto, J., Takizawa, O., Komori, M., & Takahashi, T. (2001). Measurement of in-vivo local shear modulus by combining multiple phase offsets MR elastography. *Studies in Health Technology and Informatics*, 84(February 2001), 933–937. <https://doi.org/10.3233/978-1-60750-928-8-933>
- Sugiura, Y., Sakuma, K., Sakuraba, K., & Sato, Y. (2017). Prevention of Hamstring Injuries in Collegiate Sprinters. *Orthopaedic Journal of Sports Medicine*, 5(1). <https://doi.org/10.1177/2325967116681524>
- Taş, S., Onur, M. R., Yılmaz, S., Soylu, A. R., & Korkusuz, F. (2017). Shear Wave Elastography Is a Reliable and Repeatable Method for Measuring the Elastic Modulus of the Rectus Femoris Muscle and Patellar Tendon. *Journal of Ultrasound in Medicine : Official Journal of the American Institute of Ultrasound in Medicine*, 36(3), 565–570. <https://doi.org/10.7863/ultra.16.03032>
- Thelen, D. G., Chumanov, E. S., Best, T. M., Swanson, S. C., & Heiderscheit, B. C. (2005). Simulation of biceps femoris musculotendon mechanics during the swing phase of sprinting. *Medicine and Science in Sports and Exercise*. <https://doi.org/10.1249/01.mss.0000176674.42929.de>
- Thelen, D. G., Chumanov, E. S., Hoerth, D. M., Best, T. M., Swanson, S. C., Li, L., Young, M., & Heiderscheit, B. C. (2005). Hamstring muscle kinematics during treadmill sprinting. *Medicine and Science in Sports and Exercise*.

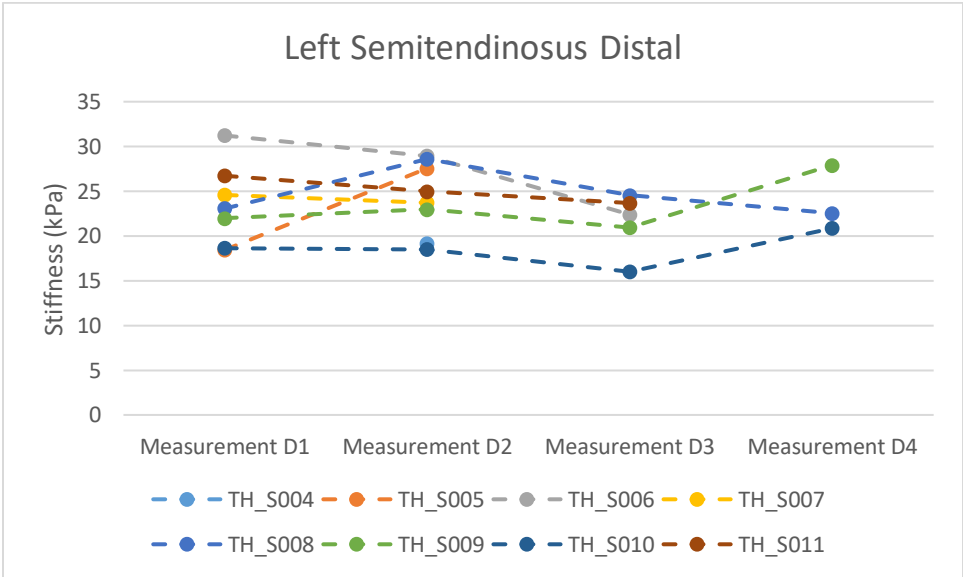
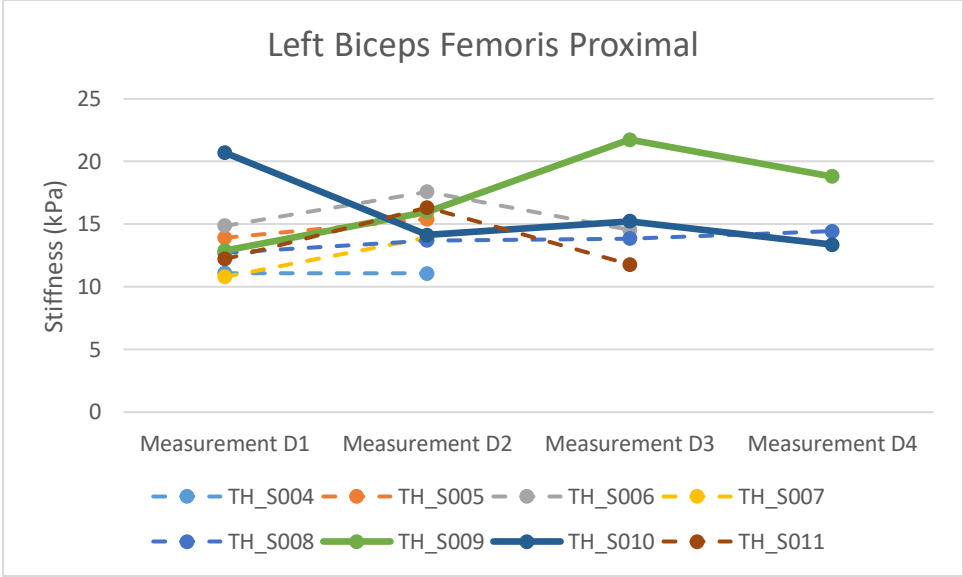
- <https://doi.org/10.1249/01.MSS.0000150078.79120.C8>
- Verrall, G. M., Slavotinek, J. P., & Barnes, P. G. (2005). The effect of sports specific training on reducing the incidence of hamstring injuries in professional Australian Rules football players. *British Journal of Sports Medicine*, 39(6), 363–368.
<https://doi.org/10.1136/bjism.2005.018697>
- Verrall, G. M., Slavotinek, J. P., Barnes, P. G., & Fon, G. T. (2003). Diagnostic and Prognostic Value of Clinical Findings in 83 Athletes with Posterior Thigh Injury. Comparison of Clinical Findings with Magnetic Resonance Imaging Documentation of Hamstring Muscle Strain. *American Journal of Sports Medicine*, 31(6), 969–973.
<https://doi.org/10.1177/03635465030310063701>
- Warren, G. L., Hayes, D. A., Lowe, D. A., & Armstrong, R. B. (1993). Mechanical Factors In The Initiation Of Eccentric Contraction-Induced Injury In Rat Soleus Muscle. *Journal of Physiology*, 464, 457–475.
- Watson, M. D., & DiMartino, P. P. (1987). Incidence of injuries in high school track and field athletes and its relation to performance ability. / Frequence des lesions chez des athletes de l'enseignement superieur et rapport avec les performances. *American Journal of Sports Medicine*, 15(3), 251–254.
<http://articles.sirc.ca/search.cfm?id=201497%0Ahttp://ezproxy.library.ubc.ca/login?url=http://search.ebscohost.com/login.aspx?direct=true&db=sph&AN=SPH201497&login.asp&site=ehost-live&scope=site%0Ahttp://www.aossm.org/>
- Whitehead, N. P., Allen, T. J., Morgan, D. L., & Proske, U. (1998). Damage to human muscle from eccentric exercise after training with concentric exercise. *Journal of Physiology*, 512(2), 615–620. <https://doi.org/10.1111/j.1469-7793.1998.615be.x>
- Winn, N., Lalam, R., & Cassar-Pullicino, V. (2016). Sonoelastography in the musculoskeletal system: Current role and future directions. *World Journal of Radiology*, 8(11), 868–879.
[https://doi.org/10.1016/S0016-7878\(84\)80013-9](https://doi.org/10.1016/S0016-7878(84)80013-9)
- Wood, S., Morgan, D. L., & Proske, U. (1993). Effects of repeated eccentric contractions on structure and mechanical properties of toad sartorius muscle. *American Journal of Physiology*, 265, C792-C800.
- Woods, C., Hawkins, R. D., Maltby, S., Hulse, M., Thomas, A., & Hodson, A. (2004). The Football Association Medical Research Programme: An audit of injuries in professional football - Analysis of hamstring injuries. *British Journal of Sports Medicine*, 38(1), 36–41.
<https://doi.org/10.1136/bjism.2002.002352>
- Xiao, Y., Zeng, J., Niu, L., Zeng, Q., Wu, T., Wang, C., Zheng, R., & Zheng, H. (2014). Computer-aided diagnosis based on quantitative elastographic features with supersonic shear wave imaging. *Ultrasound in Medicine and Biology*, 40(2), 275–286.
<https://doi.org/10.1016/j.ultrasmedbio.2013.09.032>
- Yanagisawa, O., Niitsu, M., Kurihara, T., & Fukubayashi, T. (2011). Probabilistic performance assessment for radioactive waste disposal: A simplified biosphere model. *Clinical Radiology*, 66, 815–819. <https://doi.org/10.1016/j.crad.2011.03.012>
- Yoshitake, Y., Takai, Y., Kanehisa, H., & Shinohara, M. (2014). Muscle shear modulus measured with ultrasound shear-wave elastography across a wide range of contraction intensity. *Muscle and Nerve*, 50(1), 103–113. <https://doi.org/10.1002/mus.24104>
- Zaki, R., Bulgiba, A., Ismail, R., & Ismail, N. A. (2012). Statistical methods used to test for agreement of medical instruments measuring continuous variables in method comparison studies: A systematic review. In *PLoS ONE* (Vol. 7, Issue 5).

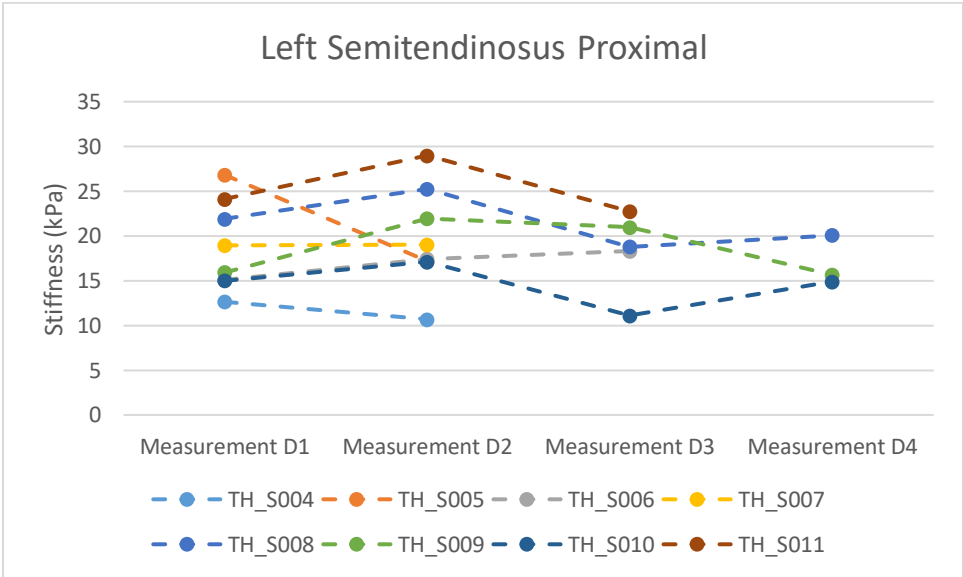
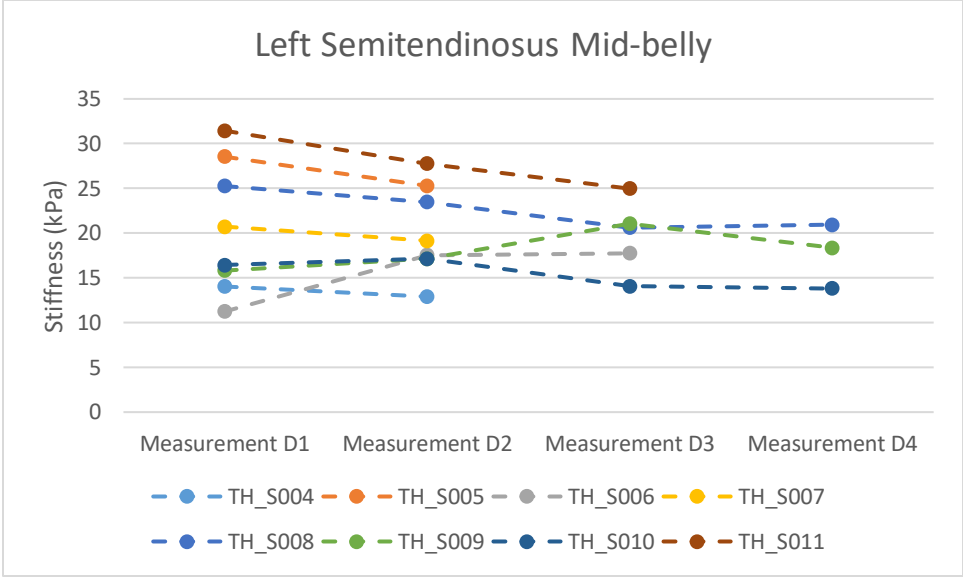
<https://doi.org/10.1371/journal.pone.0037908>

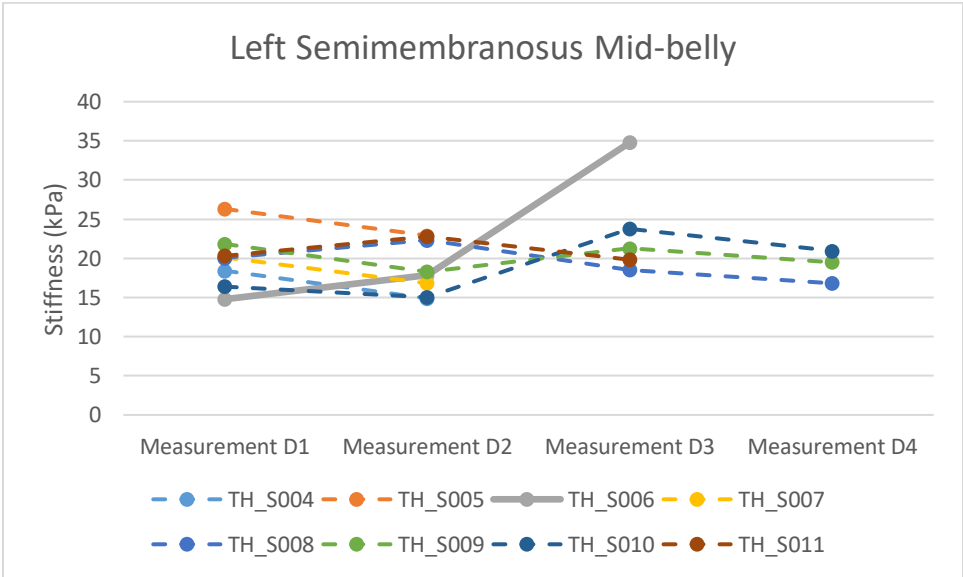
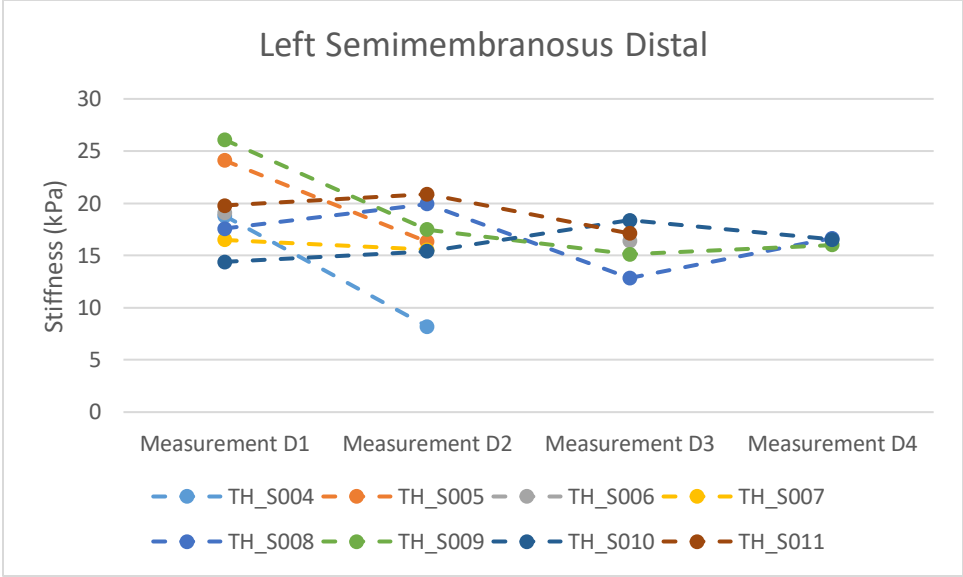
Zemper, E. D. (2005). Track and field injuries. In *Medicine and Sport Science*.
<https://doi.org/10.1159/000084287>

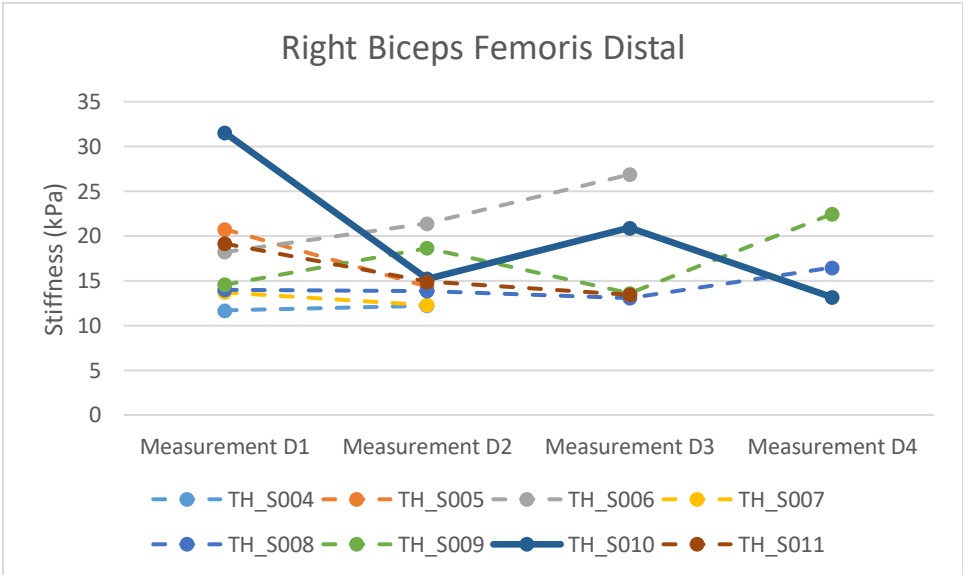
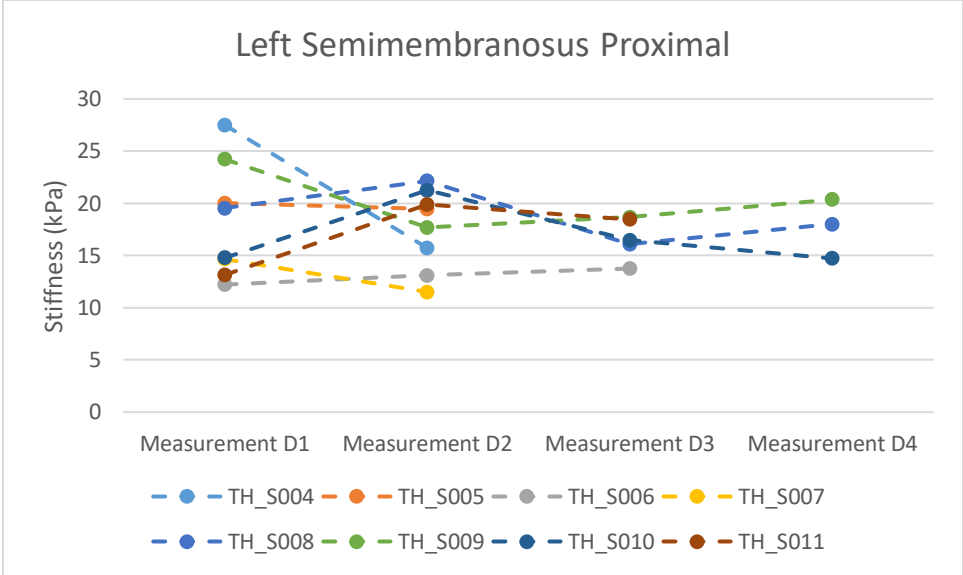
APPENDIX A: INDIVIDUAL PARTICIPANT HAMSTRING STIFFNESS PLOTS

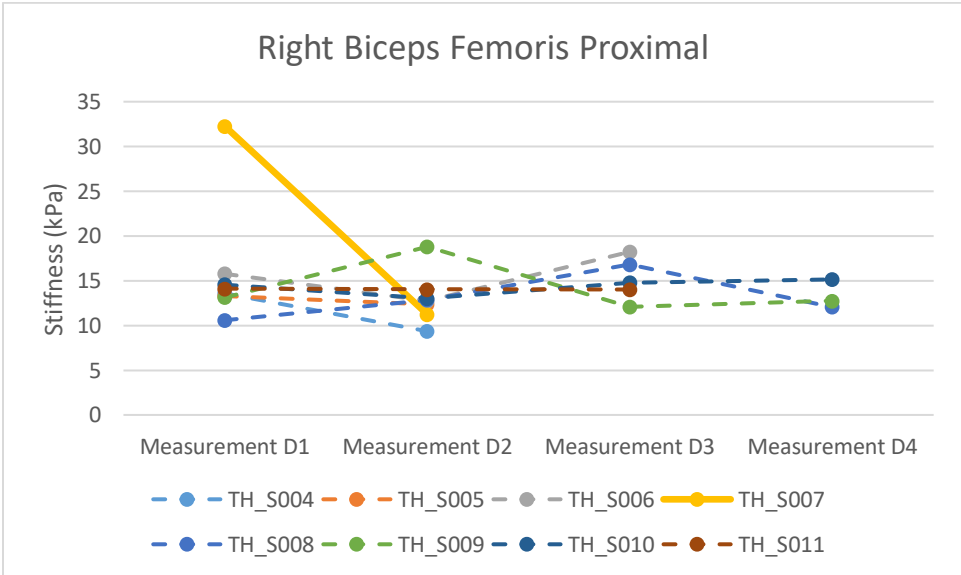
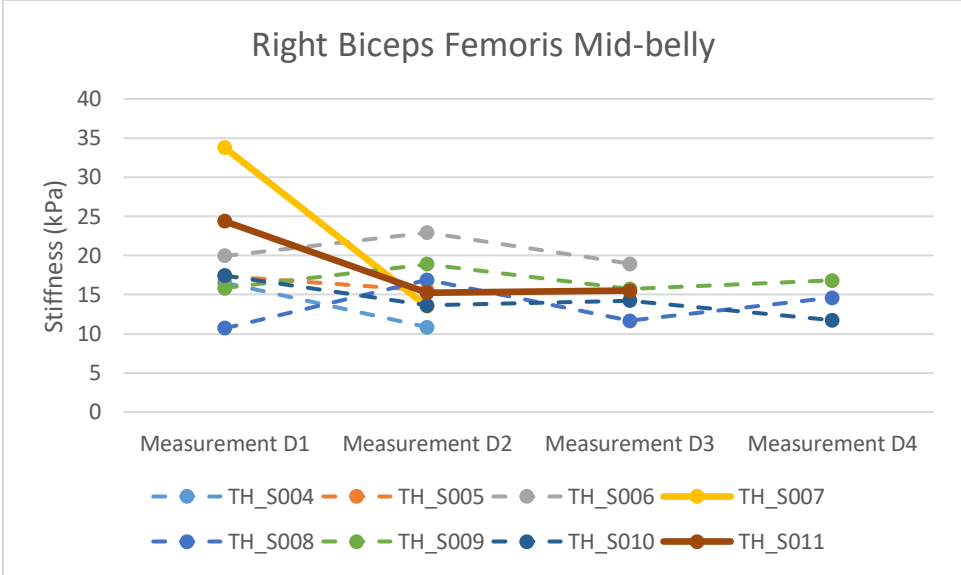


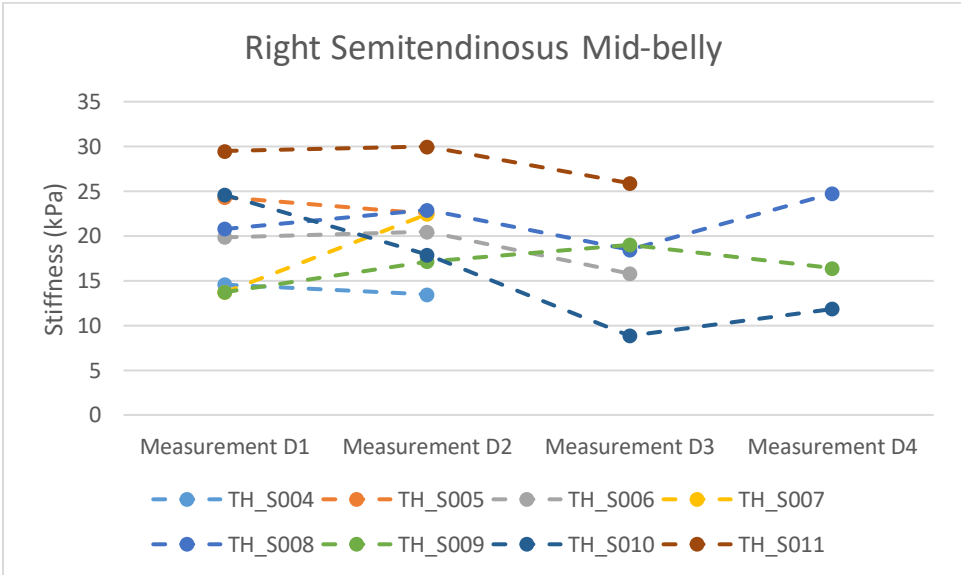
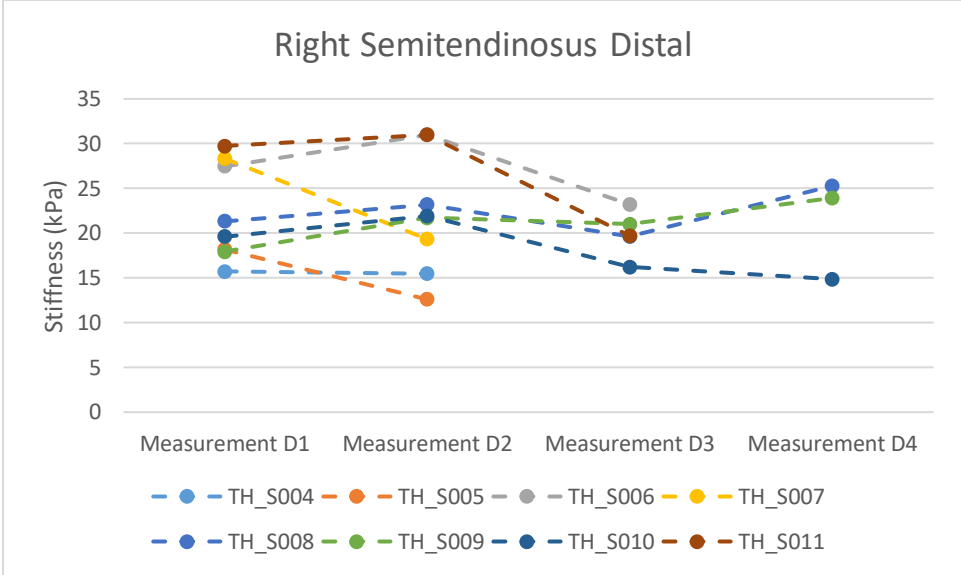


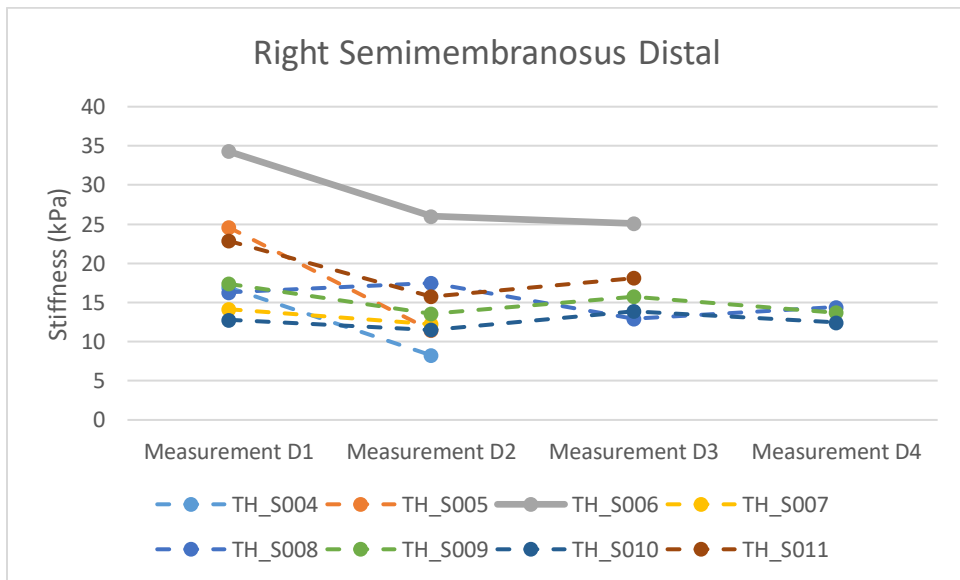
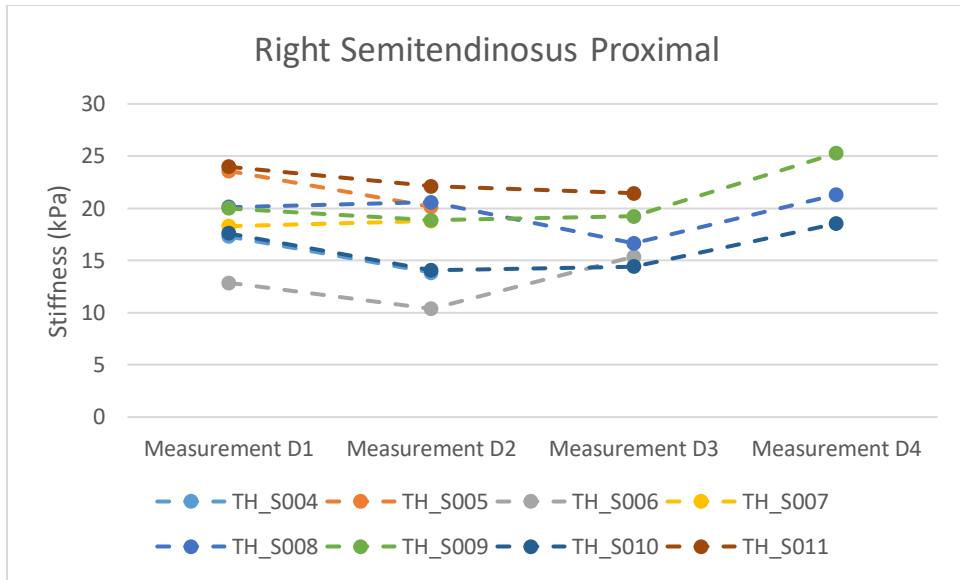


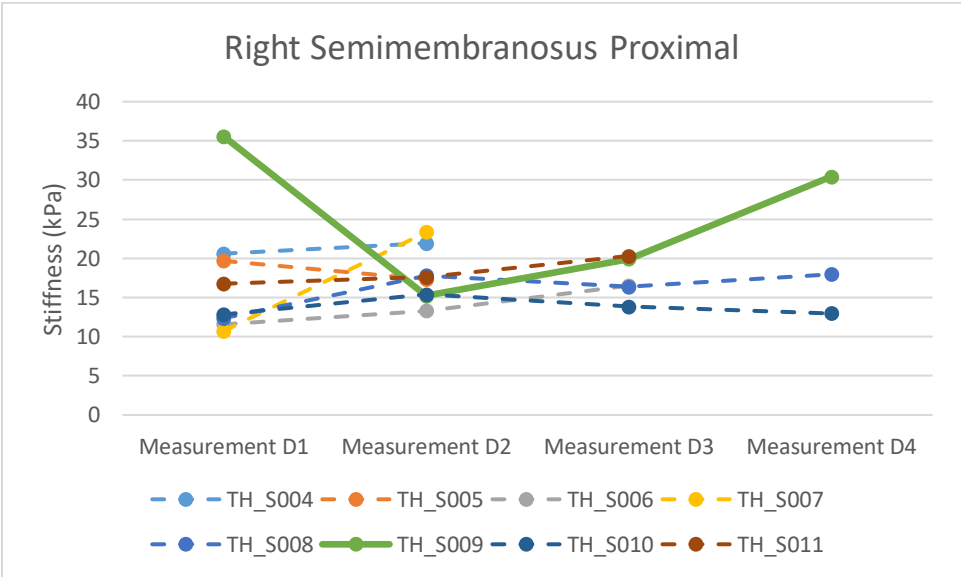
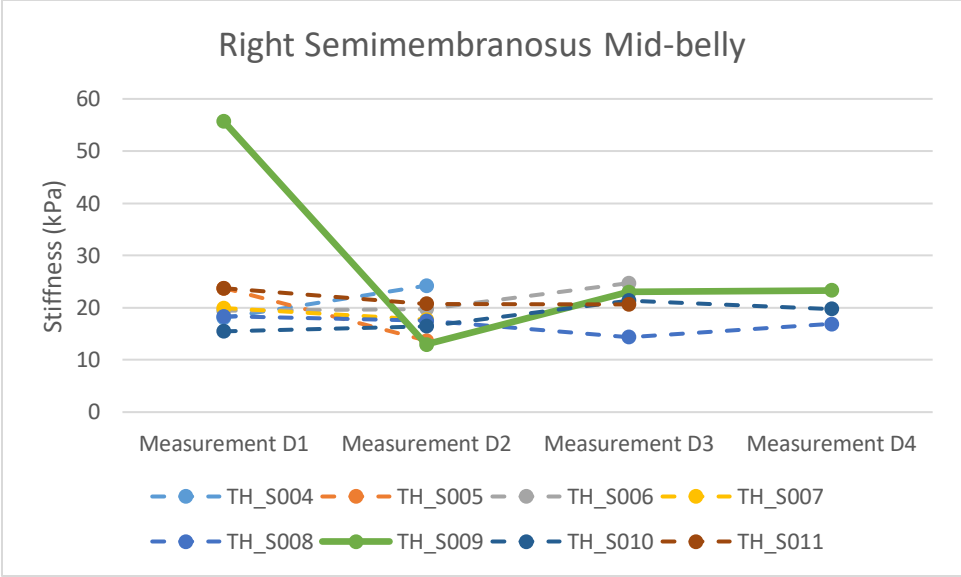












APPENDIX B: DEMOGRAPHICS QUESTIONNAIRE

Questionnaire for Ultrasound Elastography Measurements as Predictor for Hamstring Strains

1. Date of Birth: _____

2. Sex **Male** **Female**

3. What events do you compete in? (List all)

4. Do you currently have a hamstring strain injury?

Yes **No**

If yes, please specify what leg the injury occurred in, which muscle(s) the injury occurred in, and where in the muscle(s) it occurred (if possible)

5. Have you had a hamstring injury in the past?

Yes **No**

If yes, how long ago was it?

If yes, please specify what leg the injury occurred in, which muscle(s) the injury occurred in and where in the muscle(s) it occurred (if possible)

6. What is your start leg?

Right **Left**

7. What is your lead leg (if applicable)?

Right **Left**

8. What is your jumping leg (if applicable)?

Right

Left

APPENDIX C: INFORMED CONSENT DOCUMENT



Informed Consent to Participate in Research

Information to consider before taking part in research that has no more than minimal risk.

Title of Research Study: Development and Application of a Custom Algorithm to Assess Hamstring Muscle Stiffness

Principal Investigator: Zachary J. Domire, Ph.D.

Institution/Department or Division: Department of Kinesiology

Address: 332 Ward Sports Medicine Building

Telephone #: 252.737.4564

Study Sponsor/Funding Source: N/A

Researchers at East Carolina University (ECU) study problems in society, health problems, environmental problems, behavior problems and the human condition. Our goal is to try to find ways to improve the lives of you and others. To do this, we need the help of volunteers who are willing to take part in research.

Why is this research being done?

The purpose of this research is to determine if muscle stiffness is a predictor of hamstring strains. The decision to take part in this research is yours to make. By doing this research, we hope to learn if there is a correlation between muscle stiffness and the occurrence of hamstring strains.

Why am I being invited to take part in this research?

You are being invited to take part in this research because you are sprinter/jumper on the ECU track & field team and over the age of 18 years old. If you volunteer to take part in this research, you will be one of about 100 people to do so.

Are there reasons I should not take part in this research?

I understand I should not participate in this study if I am below 18 years old.

What other choices do I have if I do not take part in this research?

You can choose not to participate.

Where is the research going to take place and how long will it last?

The research procedures will be conducted in the Biomechanics Laboratory in the Ward Sports Medicine Building. You will need to come to room 332 approximately 10 times during the study. The total amount of time you will be asked to volunteer for this study 10 hours over the next 10 months.

What will I be asked to do?

You are being asked to do the following in the order presented:

1. Read and sign this informed consent form.
2. Provide personal information about your general health, injury history, and leg dominance.
3. Have your height and weight measured.
4. Have ultrasound elastography images of your hamstring muscles taken while lying in the prone position.
5. Return once per month to have steps 3 and 4 repeated.
6. If you strain your hamstring, you will be asked to come in once per week for steps 3 and 4 to be repeated until the injury appears normal on the ultrasound. (Note: this will increase the number of hours and total time you will be asked to volunteer for the study)

Ultrasound is the technique of using sound waves that are unable to be felt to create an image; much like a pregnant woman gets a sonogram to see a picture of her baby. In this case, the sound waves will be used to create an image of your muscle. Using these sound waves, we are also able to measure the stiffness of your muscle by measuring how quickly these waves travel through the tissue. This ultrasound technique is called elastography.

What possible harms or discomforts might I experience if I take part in the research?

It has been determined that the risks associated with this research are no more than what you would experience in everyday life.

What are the possible benefits I may experience from taking part in this research?

We do not know if you will get any benefits by taking part in this study. This research might help us learn more about possible risk factors for hamstring strains. There may be no personal benefit from your participation, but the information gained by doing this research may help others in the future.

Will I be paid for taking part in this research?

We will not be able to pay you for the time you volunteer while being in this study.

What will it cost me to take part in this research?

It will not cost you any money to be part of the research.

Who will know that I took part in this research and learn personal information about me?

To do this research, ECU and the people and organizations listed below may know that you took part in this research and may see information about you that is normally kept private. With your permission, these people may use your private information to do this research:

- The University & Medical Center Institutional Review Board (UMCIRB) and its staff, who have responsibility for overseeing your welfare during this research, and other ECU staff who oversee this research.
- Any agency of the federal, state, or local government that regulates human research. This includes the Department of Health and Human Services (DHHS), the North Carolina Department of Health, and the Office for Human Research Protections.

How will you keep the information you collect about me secure? How long will you keep it?

Data files will be kept for 6 years after the study is completed. We will keep your personal data in strict confidence by having your data coded. Instead of your name, you will be identified in the data records with an identity number. Your name and code number will not be identified in any subsequent report or publication. We (the study

APPENDIX D: CUSTOM ALGORITHM FLOWCHART

Figure 1.1 – Image selection and image color bar data extraction

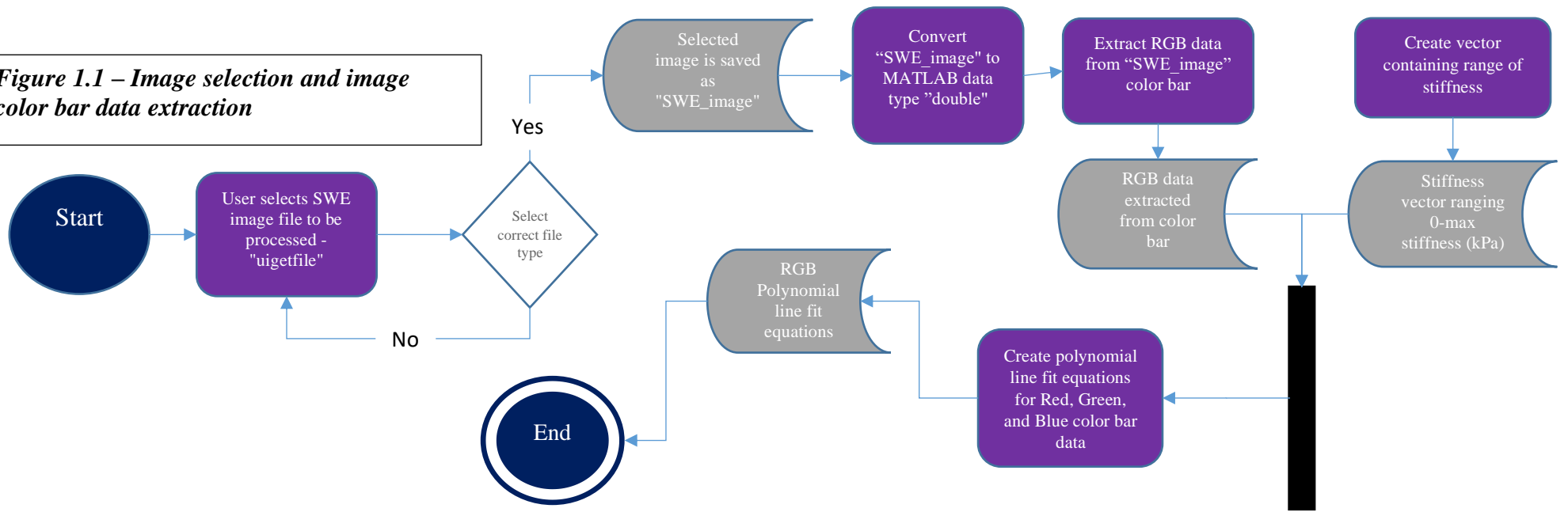


Figure 1.2 – Establish a region of interest and gather pixel intensity values

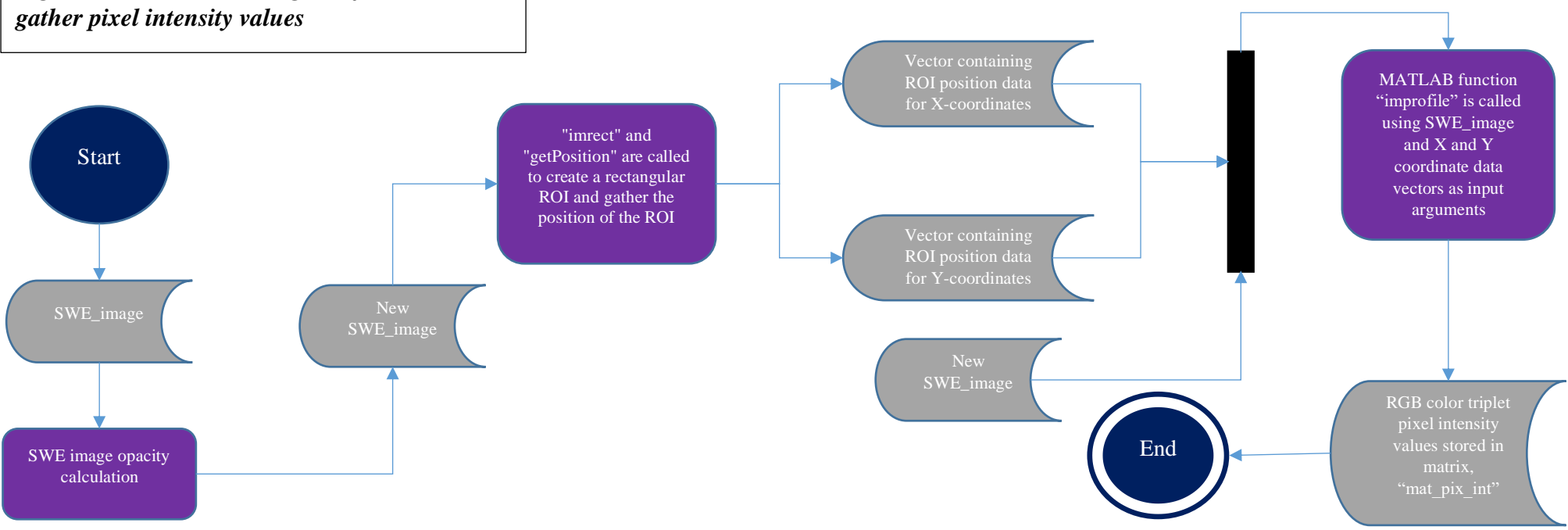


Figure 1.3 – Check that every pixel in our ROI contains valid stiffness information

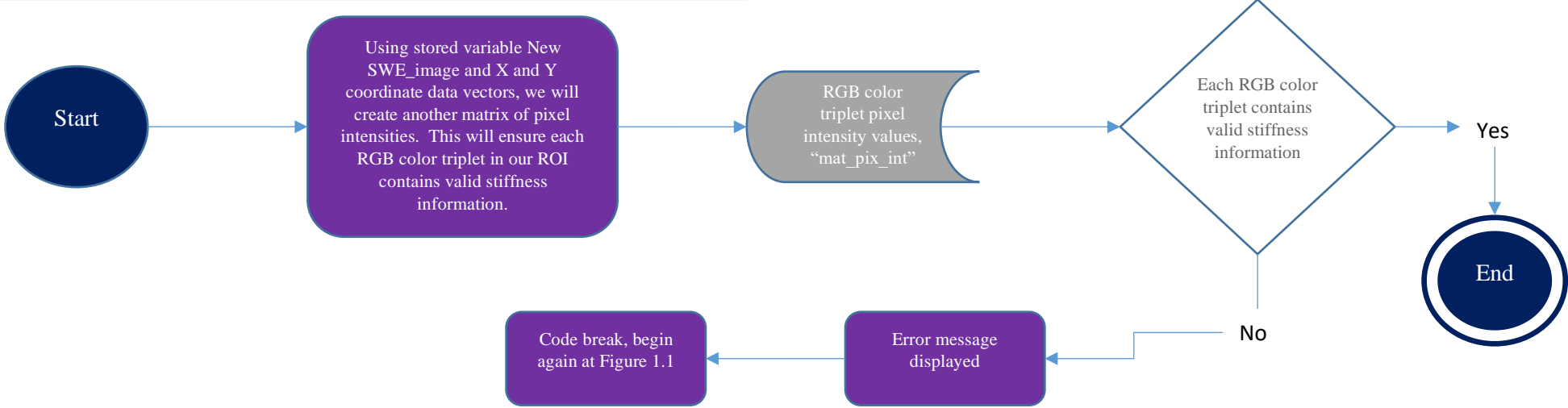
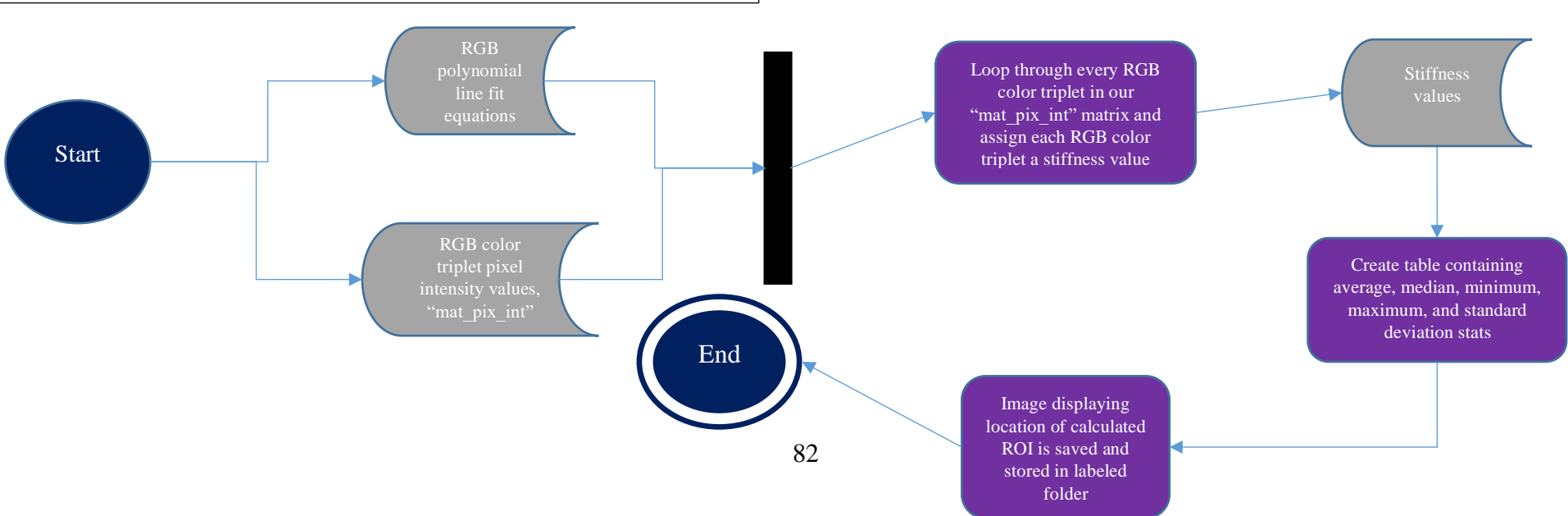


Figure 1.4 – Assign stiffness values to each RGB color triplet in ROI



APPENDIX E: IRB APPROVAL LETTER



EAST CAROLINA UNIVERSITY
University & Medical Center Institutional Review Board
4N-64 Brody Medical Sciences Building · Mail Stop 682
600 Moyer Boulevard · Greenville, NC 27834
Office **252-744-2914** · Fax **252-744-2284** · rede.ecu.edu/umcirb/

Notification of Continuing Review Approval: Expedited

From: Biomedical IRB

To: [Zachary Domire](#)

CC: [Patrick Rider](#)

Date: 4/1/2020

Re: [CR00008494](#)
[UMCIRB 14-001352](#)

Development and Application of a Custom Algorithm to Assess Hamstring Muscle Stiffness

The continuing review of your expedited study was approved. Approval of the study and any consent form(s) is for the period of 3/31/2020 to 3/30/2021. This research study is eligible for review under expedited category # 4. The Chairperson (or designee) deemed this study no more than minimal risk.

Changes to this approved research may not be initiated without UMCIRB review except when necessary to eliminate an apparent immediate hazard to the participant. All unanticipated problems involving risks to participants and others must be promptly reported to the UMCIRB. The investigator must submit a continuing review/closure application to the UMCIRB prior to the date of study expiration. The Investigator must adhere to all reporting requirements for this study.

Approved consent documents with the IRB approval date stamped on the document should be used to consent participants (consent documents with the IRB approval date stamp are found under the Documents tab in the study workspace).

The approval includes the following items:

Document	Description
Informed Consent Elastography Hamstring Study - New Template.doc(0.01)	Consent Forms
Protocol for Ultrasound Elastography Measurements as a Predictor of Hamstring Study Protocol or Grant Strains.docx(0.02)	Application
Questionnaire for Ultrasound Elastography Measurements as Predictor for Hamstring Strains.docx(0.01)	Surveys and Questionnaires

For research studies where a waiver of HIPAA Authorization has been approved, each of the waiver criteria in 45 CFR 164.512(i)(2)(ii) has been met. Additionally, the elements of PHI to be collected as described in items 1 and 2 of the Application for Waiver of Authorization have been determined to be the minimal necessary for the specified research.

The Chairperson (or designee) does not have a potential for conflict of interest on this study.

